Università di Torino

Molecular Biotechnology Center

UNIVERSITÀ DEGLI STUDI DI TORINO

Dissecting the intracellular and the extracellular functions of Morgana in triple negative breast cancer

PhD Program in Biomedical Sciences and Oncology

Laura Seclì

Novembre 2018

Sommario

Abstract

Triple Negative Breast Cancer (TNBC) is a common malignancy in woman. Despite the recent advance in diagnostic methods, the mortality for this cancer remains high. Patient death results entirely from metastasis formation in distant organs. Definitively, our possibility to control the pathology depends on our ability to block cancer metastasis by understanding the subtended molecular mechanisms. Morgana, an ubiquitously expressed protein with chaperone and co-chaperone functions, is overexpressed in 36% of TNBCs, conferring chemoresistance to cancer cells. Here we show, that Morgana finely control other important features of cancer progression. In particular, we demonstrated that Morgana binds to the IKK complex and is essential for NF-κB activation. High Morgana expression levels in cancer cells inhibit natural killer cell recruitment in the first phases of tumor growth and induce the expression of cytokines able to attract neutrophils in the primary tumor, as well as in the pre-metastatic lungs, fueling cancer metastasis. In addition, we demonstrated that Morgana is actively and unconventionally secreted by TNBC cell lines and not by normal cells. Once outside, eMorgana promotes cell migration in an autocrine manner, binding to TLR2 and TLR4. Hence, eMorgana could represent a biomarker in the serum of breast cancer patients and a targetable protein to treat TNBC.

Introduction

Morgana is a protein containing two CHORD (cysteine and histidine rich) domains able to coordinate Zn^{++} ions and a C-terminal CS (after CHORD-containing proteins and Sgt1) domain [1], homologous to the small chaperones α-crystallin and p23 [2]. CHORD domains are phylogenetically conserved from plants to mammals. The first CHORD containing protein identified was the plant protein RAR1, involved in disease resistance signaling [1]. In metazoan and fungi CHORD containing proteins (Chps) acquired the CS domain, with the exception of yeast, that does not possess Chps [1]. While not vertebrates hold a single Chp coding gene, in vertebrates two genes are present, coding for Morgana and Melusin [3, 4]. Mammalian Chps share the 63% homology in the amino acid sequence and a similar domain structure.

While Melusin expression is restricted to skeletal muscle and myocardium [3-5], Morgana is ubiquitously expressed. Both proteins have been described to bind to HSP90 [6-12], that is one of the best studied molecular chaperones in eukaryotes, accounting for the 2% of the total cytosolic protein content. The chaperone HSP90 interacts with two different classes of proteins: co-chaperones, able to assist and coordinate the HSP90 cycle and more than 200 substrate proteins, also known as clients, depending on HSP90 for their stabilization and activation. A number of co-chaperone proteins have been identified and described to associate dynamically with HSP90 during its chaperone cycle, among them SGT1, PP5, p23, prolylisomerase, Hop, Cdc37, Melusin and Morgana [13]. Morgana, as other HSP90 co-chaperones [14], displays an HSP90 independent molecular chaperone activity in suppressing the aggregation of denatured proteins and when overexpressed protects cells from apoptosis induced by different stress stimuli, like heat shock and hydrogen peroxide [9].

Due to their capacity to fold and refold proteins when these are defective or irreversibly misfolded [15, 16] and to their roles in regulating cellular processes from gene expression to signal transduction [17], chaperones and co-chaperones are considered important players in cancer progression.

Levels of HSPs are aberrantly high in human cancers compared to their normal tissues of origin and may correlate with poor prognosis [18, 19]. Indeed HSPs have been implicated in the maintenance of sustained proliferative signaling, resisting cell death, inhibition of replicative senescence, induction of tumour angiogenesis, activation of invasion and metastasis, reprogramming of energy metabolism and evasion of immune destruction [20]. For example

among HSP90 clients there are several proteins involved in cancer survival, such as human epidermal growth factor receptor 2 (HER2), AKT, c-Met, and HIF-1α, as well as steroid hormone receptors and mutant oncoproteins (p53 and B-Raf) and immune regulators (IRF and NF-κB) [21, 22].

The relation between the heat shock response and the inflammatory process is known by different decades [23] and is not a case that both mechanisms are fundamental in controlling cellular response and homeostasis during a danger stimulus in order to avoid cell death [24]. Although controversial studies and opinions exist in the field, we can say that the regulation between these two processes is not univocal. Indeed if on the one hand HSPs can directly affect inflammatory pathways inside the cell, on the other hand inflammatory cytokines can control HSPs expression acting on HSF-1 (heat shock factor-1), the master regulator of chaperone transcription [25-27]. One can conclude that the role of HSPs in cancer could be also linked to their capacity to modulate immune genes since it is well described the relationship between chronic inflammation and tumour progression.

Bidirectional communication between cells and their microenvironment is critical both for normal tissue homeostasis and for tumour growth. In particular, the tumour associated stroma, that contains "corrupted" cells belonging to the mesenchymal, vascular and immune tissues, can influences disease initiation, progression and finally patient prognosis [28]. For this powerful relationship with the surrounding microenvironment, tumours were addressed as "wounds that never heals" [29], comparing them to parasites that evoke the wound-healing response to acquire the stroma they need for survival and growth. As in wound repair, inflammatory cells are key players in tuning cellular processes in tumour lesions. After the initial recognition of transformed cells by immunological effector cells, an equilibrium phase is reached between malignant cells and the immune reaction that is unfortunately followed by a final escape of cancer cells from immunological control. This leads to the selection of nonimmunogenic cancer cells (immunoediting) or active suppression of the local immune response (immunosubversion) [30]. Moreover, if it is true that cancer cells can encounter oncogenic changes that lead to the modulation of inflammatory pathways, it is well established also the contrary. Indeed chronic inflammation associated with infections or autoimmune disease favors tumour development and can contribute to it through induction of oncogenic mutations, genomic instability, early tumour promotion, and enhanced angiogenesis [31]. As a result of these different forms of inflammation, the tumour microenvironment contains innate immune cells (including macrophages, neutrophils, mast

cells, myeloid derived suppressor cells, dendritic cells, and natural killer cells) and adaptive immune cells (T and B lymphocytes) in addition to the cancer cells and their surrounding stroma (which consists of fibroblasts, endothelial cells, pericytes, and mesenchymal cells) [32]. The active secretion of chemokines, cytokines and other modulatory molecules in the tumour microenvironment and the consequent establishment of positive and negative loops among all these players begin essential to sustain tumour progression and aggressiveness [32].

The data obtained by our study lead us to the identification of a dual role of Morgana in breast cancer. Indeed, if on the one hand Morgana is able to induce tumour progression through the activation of NF-κB and the consequent modulation of the tumour microenvironment [33], on the other hand Morgana is secreted by breast cancer cells and exerts an autocrine modulation of TLR2 and TLR4, favoring cancer cell migration (in preparation).

Breast cancer is the most common cancer in women worldwide and it is the second leading cause of cancer-related death in women [34]. Triple-negative breast cancer (TNBC), which accounts for approximately 10%-15% of diagnosed breast cancers [35], does not express estrogen and progesterone receptors and is also negative for HER2 (Human epidermal growth factor receptor 2) overexpression [36, 37]. Compared with the hormone receptor-positive breast cancers, TNBC has a worse prognosis, with an aggressive natural history and a great propensity for lung and brain metastasis [35, 38]. Contrary to the initial belief that TNBC would be synonymous with basal-like breast cancer, Lehmann et al. [39] demonstrated the existence of six transcriptional TNBC subtypes: basal-like 1 (BL1), basal-like 2 (BL2), immunomodulatory (IM), mesenchymal (M), mesenchymal stem-like (MSL), and luminal androgen receptor (LAR), then reduced to 4 since follow-up studies by Lehmann and colleagues provided evidence that the IM and MSL subtypes are not truly representative of the biology of TNBCs [40]. Women with triple-negative breast cancer do not benefit from endocrine therapy or trastuzumab (since the absence of receptors mentioned before) and chemotherapy is currently the mainstay of systemic medical treatment [41]. Consequently, TNBCs patients undergo combination therapies, consisting mainly of surgery, radiation and chemotherapy while newly developed targeted therapy and immunotherapy are still in clinical trials. The regiments of adjuvant/neoadjuvant chemotherapy include anthracyclines, taxanes and/or platinum compounds, dose-dense doxorubicin/cyclophosphamide (AC) and docetaxel/cyclophosphamide (TC) and radiation therapy should follow chemotherapy when indicated. The role of targeted therapy as well as immunotherapy is currently under

investigation. Targeting the androgen receptor is an exciting area of research, as TNBC expressing the androgen receptor may behave with a less aggressive phenotype (LAR subtype), with a more indolent disease course. A phase II trial explored enzalutamide in androgen receptor positive advanced TNBC [42]. Another novel therapy for advanced metastatic breast cancer is olaparib, an oral poly(adenosine diphosphate-ribose) polymerase (PARP) inhibitor. In the randomized phase III trial comparing olaparib monotherapy to standard chemotherapy in metastatic germline BRCA mutant pre-treated advanced breast cancer, patients receiving olaparib arm had a significantly higher median progression free survival (PFS) compared with the chemotherapy arm [43]. For years, TNBC was not considered as a cancer eligible to immunotherapy but nowadays it is emerging as an important treatment option. From this point of view, TNBC heterogeneity is maintained and this breast cancer is divided into five immune subtypes based on four distinct expression signatures: T/Bcell/IFN high, IFN/CSR (macrophages) high, CSR high, TGFβ high and immune low [44]. On this line, anti PD-1 and anti PD-L1 mAbs, that have been shown to be effective in the treatment of several other cancers, are unsatisfactory as single therapeutic agents in TNBC [45]. For this reason, different PD-1 and PD-L1 inhibitors are under investigation in combination regimens with chemotherapy and other targeted agents, including tyrosine kinase inhibitors, MEK inhibitors, PI3-K inhibitors, anti-angiogenic agents, PARP inhibitors or co-stimulatory molecules [45]. However due to genomic complexity, tumour heterogeneity and clonal evolution of TNBC, further research is needed to develop strategies to overcome resistance and develop a rational combination of different therapies to treat patients in safety.

Aberrant activation of NF-κB is frequently found in triple-negative breast cancer (TNBC) [46]. The family of NF-κB transcription factors consists of five members, RelA/p65, c-Rel, RelB, NF-κB1 (p50), and NF-κB2 (p52), forming homo- and heterodimers. In absence of specific stimuli, these dimers are bound to IκB (inhibitors of NF-κB) and are kept transcriptionally inactive. The NF-κB signaling pathway responds to different stimuli, from cytokine and growth factor signaling to the recognition of pathogen products or DNA damages and oncogenic stress. The activation of the NF-κB "canonical pathway" induces the formation of the IKK (IκB kinase) protein complex containing the IKKα and IKKβ kinases and the regulatory subunit IKKγ/NEMO. The activated IKK complex phosphorylates IκBα inducing its detachment from NF-κB and its degradation. As a result, NF-κB dimers can enter the nucleus and regulate the transcription of their target genes [47]. NF-κB is involved in activating immune and inflammatory responses but also in regulating adhesion, angiogenesis,

autophagy, energy metabolism, senescence, and inducing cell proliferation and survival [48, 49]. It is therefore not surprising that NF-κB has been involved in cancer onset and progression both in experimental models and in human patients [50, 51]. We found that Morgana is a previously unknown component of the IKK complex. Although Morgana is not required for IKK complex formation, is essential for the recruitment of IκBα to the IKK complex and ultimately for its phosphorylation, and for NF-κB downstream activation. NF-κB target genes include cytokines, chemokines and soluble factors that once secreted can shape immune cell recruitment both in the tumour and in distant organs. In particular, we showed that in the first phases of tumour growth Morgana inhibits Natural Killer (NK) cell recruitment and later, it recruits neutrophils that favor disease progression, shaping the composition of the immune-cell infiltrate in the primary tumour and in the lung pre-metastatic niche.

Signaling molecules actively secreted by tumour cells include growth factors, enzymes such as proteases, smaller protein molecules like chemokines and cytokines, as well as many other proteins that act in an autocrine or paracrine fashion, resulting in the acquisition of a favourable milieu for the progression of the malignancy [28]. In particular, stressed as well as tumour cells can release a pleteora of mediators, termed damage-associated molecular patterns (DAMPs), which potently trigger inflammation. DAMPs represent a large range of chemically unrelated mediators entities such as High Mobility Group Box 1 (HMGB1), S100 proteins, hyaluronan, HSPs, ATP and calreticulin that are retained inside the cell in the healthy state and only released following stress [52]. Normally, DAMPs warn the body about the presence of tissue injury and in the setting of infection, and thereby trigger more profound immune responses. In analogy, premalignant or malignant cells, secreting DAMPs, initially trigger an acute inflammation with a potent anti-tumour response, leading to a chronic unresolved inflammation with a tumour-promoting effect, favoring carcinogenesis in many settings [52]. Due to the loss of a signal peptide in their sequence, all these proteins reach the stroma using alternative mechanisms, avoiding the classical ER-Golgi pathway [53]. In the medium, DAMPs can act on cancer and immune cells via pattern recognition receptors (PRRs) such as Toll-like receptors (TLRs), in particular TLR2 and TLR4, and activate pro-inflammatory signaling and transcription [52]. In particular, extracellular HSPs, binding to cell surface receptors as TLR2 and TLR4, CD91, CD40, CCR5 and scavenger receptors [54], influence different steps of cancer progression, including cell proliferation, migration and invasion, vascular and immune modulation [55-65].

In line with this, we recently discovered that Morgana is secreted by a number of human and mouse highly aggressive breast cancer cells through an active unconventional pathway and that when secreted it induces cancer progression by activating membrane receptors on cancer cells.

Selected DAMPs and extracellular proteins, that contribute to a tumour-promoting microenvironment, have a potential clinical utility as diagnostic or prognostic biomarkers or as therapeutic targets, for instance through the use of monoclonal antibodies (mAbs) [66-68]. In the case of eMorgana we are collecting very encouraging preliminary results, but, other studies are needed to better characterize the role of eMorgana in immune regulation and to dissect the mechanism by which it exerts its pro-tumorigenic function from the outside.

Results

The IKK/NF-κB signaling pathway requires Morgana to drive breast cancer metastasis

Morgana is essential for TNBC cell invasion and metastasis

Morgana is overexpressed in the 36% of TNBC and its expression correlates positively with tumour grade, mitosis number, mean Ki67 labelling index and lymph node involvement [69]. Accordingly, Morgana is expressed at higher levels in MDA-MB-231 and BT549 human TNBC cell lines compared to non-invasive MCF7 cancer cells and MCF10A normal breast cells (Fig. 1a). We performed parallel experiment in MDA-MB-231 and BT-549 but for simplicity only the first will be shown. Silencing Morgana in MDA-MB-231 cell line using two different shRNAs (shMORG1 and shMORG2 Fig. 1b), we have not observed any differences in *in vitro* proliferation (Fig. 1c) but a significant reduction in the invasive capacity in Matrigel-coated transwell assays compared to control cells (Fig. 1d). Consistently, Morgana down-modulation significantly affected the anchorage-independent growth ability of MDA-MB-231 in a soft agar assay (Fig. 1e). All these data suggested an involvement of Morgana in the regulation of different steps of the metastasis cascade.

To validate these findings *in vivo*, MDA-MB-231 cells were injected in the tail vein of NOD/SCID/IL-2Rγc null (NSG) mice. After 4 weeks all the mice receiving MDA-MB-231 infected with empty vector exhibited macrometastases and numerous micrometastases in lungs, liver, kidneys, and heart; while only few and small micrometastases were found in the lungs of mice receiving MDA-MB-231 shMORG cells (Fig. 1f–i). To investigate the role of Morgana expression in cancer cell metastasis from primary tumours, NSG mice were inoculated subcutaneously with MDA-MB-231 shMORG cells or infected with an empty vector. While no differences were detected in primary tumour growth (Fig. 1j), after 5 weeks MDA-MB-231 infected with the empty vector formed macrometastases in the lungs, conversely cells downregulated for Morgana did not form any macrometastases and only few micrometastases were detected (Fig. 1k–m).

Morgana silencing in TNBC cells reduces MMP9 expression

The notion that metalloproteinases (MMP) mediate ECM degradation and lead to cancer cell invasion and metastasis is considered a guiding principle in cancer and in particular MMP9 is essential for invasion of TNBC cells [70, 71].

In this line, in the attempt to explain Morgana capability to induce invasion and metastasis formation, we analyzed metalloproteinase activity in MDA-MB-231 cell line. Zymography assays indicated that both extracellular and intracellular MMP9 activity were strongly impaired in MDA-MB-231 cells silenced for Morgana compared with control cells (Fig. 2a,

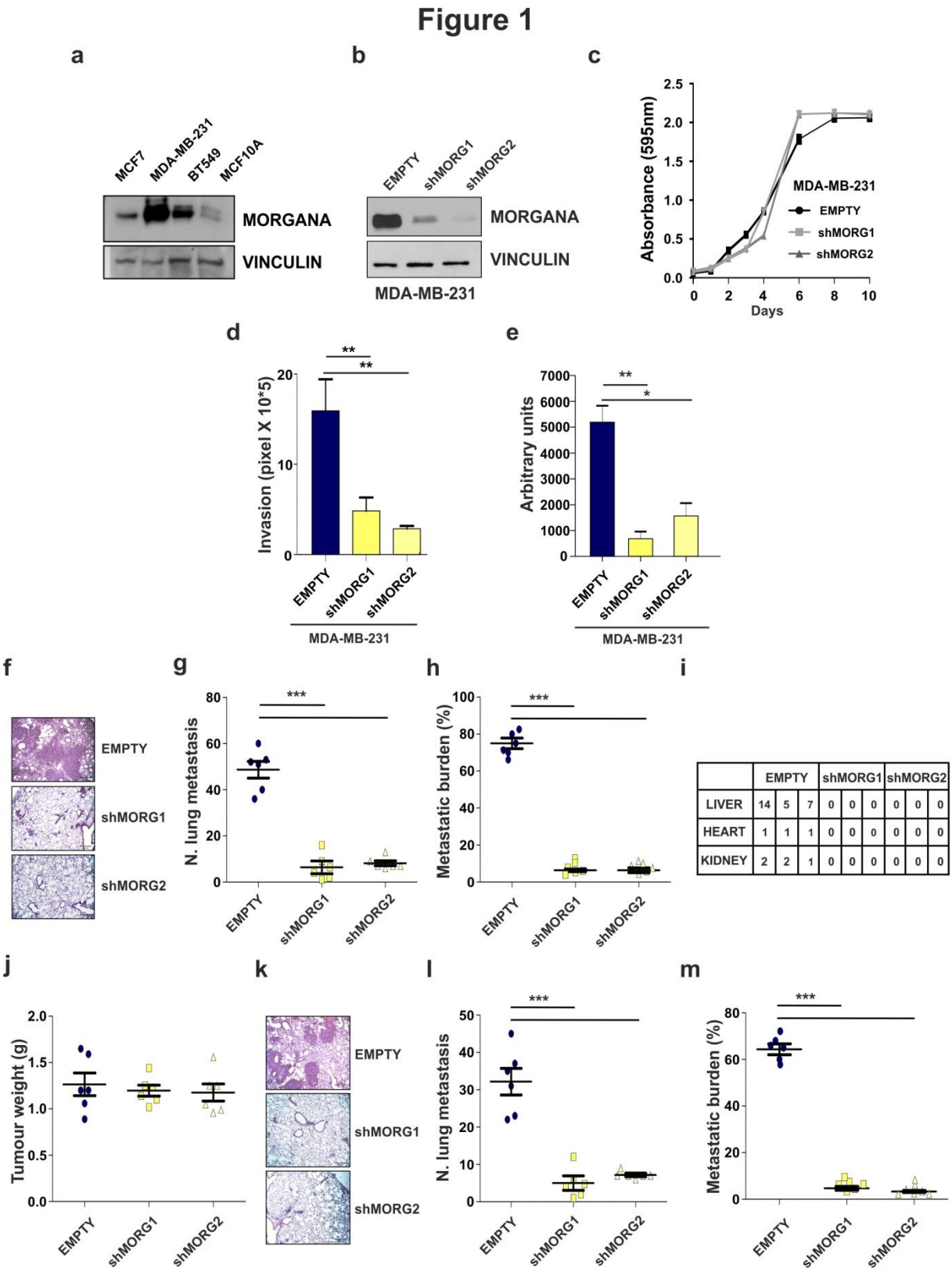

Figure 1

Morgana is essential for TNBC cell invasion and in vivo metastasis formation. **a** Immunoblotting of Morgana and Vinculin, as loading control, in MCF7, MDA-MB-231, BT549 and MCF10A cell lines. **b** Immunoblotting of Morgana and Vinculin in MDA-MB-231 cells infected with empty vector (EMPTY) or two independent Morgana shRNAs (shMORG1, shMORG2). **c** Growth curves of MDA-MB-231. **d** Quantification of invasion assays performed on MDA-MB-231 EMPTY or shMORG1 and shMORG2. **e** Quantification of soft agar colony formation by MDA-MB-231 EMPTY or shMORG1 and shMORG2. **f**–**h** Representative haematoxylin and eosin stained sections **f**, quantification of **g** pulmonary metastases and **h** metastatic burden, 4 weeks after tail vein injection of MDA-MB-231 EMPTY or shMORG1 and shMORG2 ($n = 6$ NSG mice per group). **i** Metastasis quantification in distant organs in mice injected with MDA-MB-231 EMPTY or shMORG1 and shMORG2 ($n = 3$ NSG mice per group). **j** Tumor weight 5 weeks after subcutaneous injection of MDA-MB-231 EMPTY or shMORG1 and shMORG2 ($n = 6$ NSG mice per group). **k**–**m** Representative haematoxylin and eosin stained sections **k**, quantification of **l** pulmonary metastases and **m** metastatic burden of MDA-MB-231 EMPTY or shMORG1 and shMORG2 ($n = 6$ NSG mice per group). Data are the results of at least three independent experiments. Bars in graphs represent standard errors (*$p < 0.05$; **$p < 0.01$; ***$p < 0.001$)

b). Moreover, Western blot analysis of extracellular and intracellular MMP9 revealed a relevant decrease in MMP9 expression in Morgana downregulated cells (Fig. 2c, d). Real-time PCR analysis demonstrated that Morgana downregulation affects specifically MMP9 mRNA levels while no differences were observed for MMP2 (Fig. 2e). Since MCF10A and MCF7 cells express low Morgana levels if compared with MDA-MB-231 (Fig. 1a) and a very low level of MMP9 mRNA, we overexpressed Morgana in these cell lines and we observed a significant increase in MMP9 transcription (Fig. 2f, Morgana overexpression and all annexed experiments were performed in parallel in MCF10A and MCF7, but for simplicity only those concerning MCF7 will be shown). Of note, MMP9 overexpression rescued invasion abilities in MDA-MB-231 downregulated for Morgana (Fig. 2g).

NF-κB is responsible for Morgana dependent metastasis

NF-κB and AP-1 are the most important transcription factors known to induce MMP9. To evaluate if Morgana can influence their activity we used a luciferase reporter gene with specific AP-1 or NF-κB binding sites in the promoter region. While Morgana downregulation significantly decreased NF-κB, but not AP-1 transcriptional activity in MDA-MB-231 (Fig. 3a), its overexpression in MCF7 induced a specific increase of NF-κB dependent luciferase activity (Fig. 3b). In accordance, Morgana silencing in MDA-MB-231 induced a significant reduction in the expression of several NF-κB target genes (Fig. 3c) and conversely, Morgana overexpression in MCF7 caused an increase in their expression levels (Fig. 3d). Further, Gene Ontology enrichment on data obtained in a microarray analysis (GEO ID: GSE86463), indicated that genes downregulated in MDA-MB-231 silenced for Morgana vs. control cells are mainly involved in inflammation and immune system regulation (Fig. 3e). To determine if Morgana dependent metastasis formation *in vivo* was due to NF-κB activation, we expressed an IκBα shRNA or an empty vector in MDA-MB-231 in which Morgana was downregulated (Fig. 3f). As expected, IκBα silencing induced NF-κB activation as demonstrated by a luciferase assay (Fig. 3g).

Figure 2

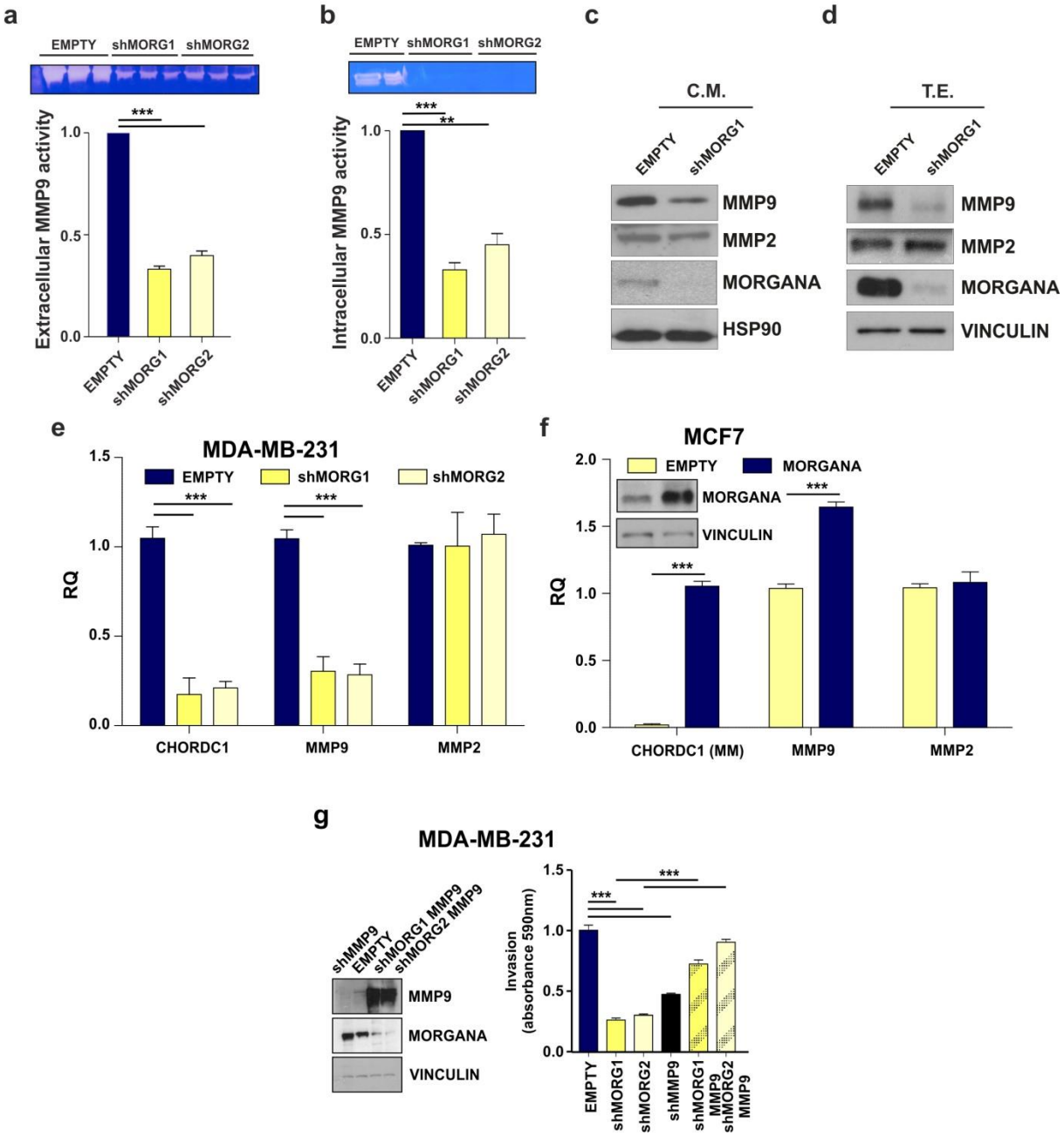

Figure 2

Morgana silencing in TNBC cells reduces MMP9 expression. **a**, **b** Extracellular **a** and intracellular **b** MMP9 activity in MDA-MB-231 infected with an empty vector (EMPTY) or shRNAs targeting Morgana (shMORG1 and shMORG2) was evaluated by gelatin zymography. Top panel: representative zymogram of MMP9 activity (92 kDa). Bottom panel: quantification of MMP9 activity from 3 independent experiments. **c** Western blot analysis of conditioned medium (C.M.) obtained from MDA-MB-231 EMPTY or shMORG1 immunostained with MMP9, MMP2, Morgana and extracellular HSP90 as loading control. Morgana, as other chaperone proteins, can be secreted by cancer cells. **d** Western blot analysis of total protein extracts (T.E.) from MDA-MB-231 EMPTY and shMORG1 immunostained for MMP9, MMP2, Morgana and Vinculin as loading control. **e** Gene expression analysis by Real-time PCR of MMP9, MMP2 and CHORDC1 (Morgana coding gene) in MDA-MB-231 EMPTY or shMORG1 and shMORG2. **f** Gene expression analysis by Real-time PCR of MMP9, MMP2 and CHORDC1 (Morgana coding gene) in MCF7 overexpressing Morgana (MORGANA) or control cells (EMPTY). **g** Quantification of invasion assays performed on MDA-MB-231 EMPTY or shMORG1 and shMORG2 infected or not with a lentiviral vector coding for MMP9 (shMORG1 MMP9, shMORG2 MMP9) or a shRNA targeting MMP9 (shMMP9). Data are the results of at least three independent experiments. Bars in graphs represent standard errors (**$p < 0.01$; ***$p < 0.001$)

Figure 3

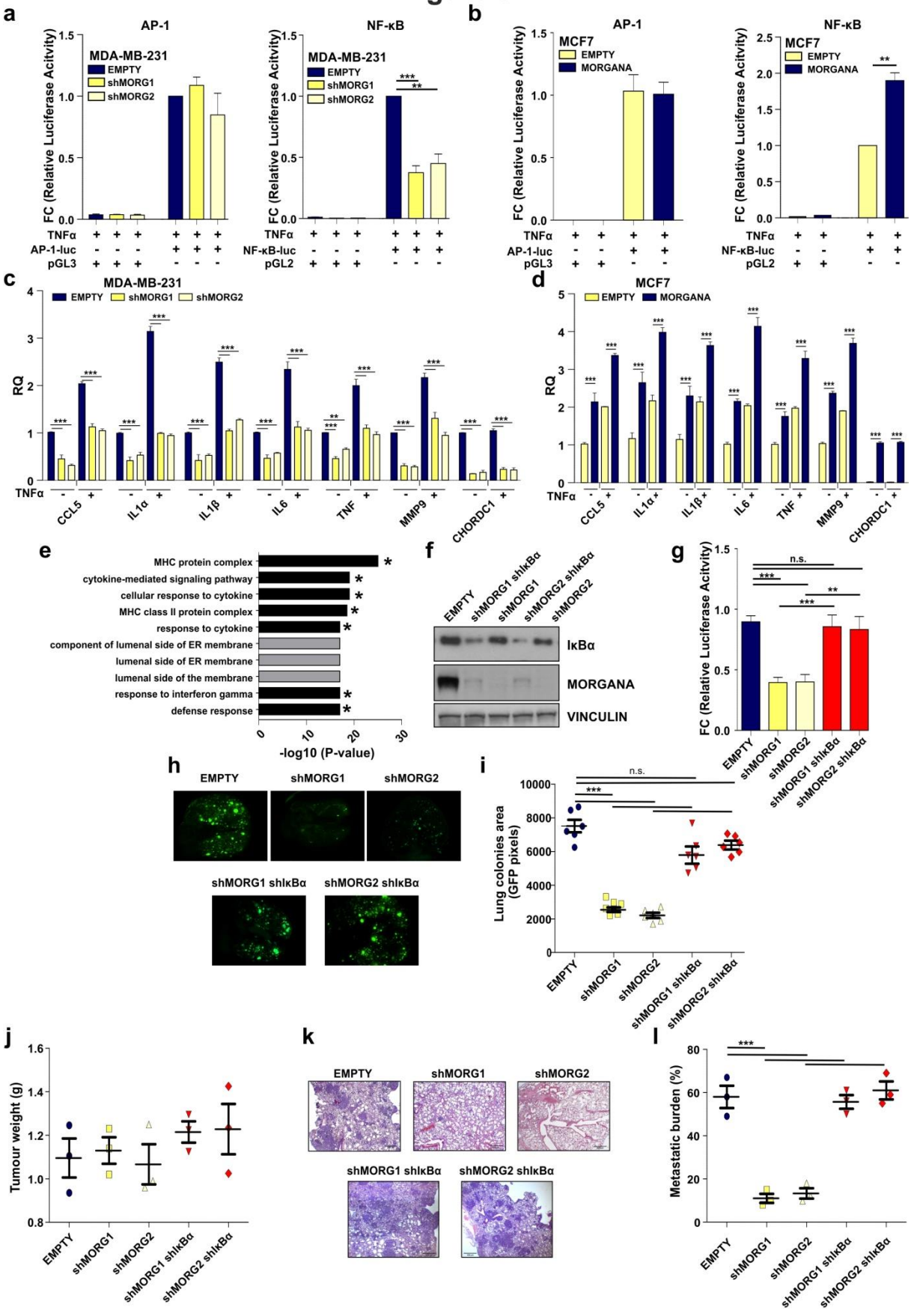
a
AP-1
NF-κB
MDA-MB-231
EMPTY
shMORG1
shMORG2
FC (Relative Luciferase Acitvity)
TNFα
AP-1-luc
NF-κB-luc
pGL3
pGL2
b
MCF7
MORGANA
c
RQ
CCL5
IL1α
IL1β
IL6
TNF
MMP9
CHORDC1
d
e
MHC protein complex
cytokine-mediated signaling pathway
cellular response to cytokine
MHC class II protein complex
response to cytokine
component of lumenal side of ER membrane
lumenal side of ER membrane
lumenal side of the membrane
response to interferon gamma
defense response
-log10 (P-value)
f
shMORG1 shIκBα
shMORG2 shIκBα
IκBα
MORGANA
VINCULIN
g
n.s.
h
i
Lung colonies area (GFP pixels)
j
Tumour weight (g)
k
l
Metastatic burden (%)

Figure 3

NF-κB pathway is responsible for Morgana dependent cancer cell metastasis. **a**, **b** Luciferase assays of AP-1 (left) and NF-κB (right) activity in **a** MDA-MB-231 infected with an empty vector (EMPTY) or shRNAs targeting Morgana (shMORG1 and shMORG2) and **b** MCF7 infected with an empty vector (EMPTY) or overexpressing Morgana (MORGANA). Cells were transfected with an AP-1 or NF-κB luciferase reporter or a control vector. **c**, **d** Gene expression analysis by Real-time PCR of NF-κB target genes in **c** MDA-MB-231 EMPTY or shMORG1 and shMORG2, and **d** MCF7 EMPTY or MORGANA, treated or not with 10nM TNFα for 4 h. **e** The top 10 gene ontology (GO) terms by enrichment P-value among the down-regulated genes obtained in a microarray analysis of MDA-MB-231 cells silenced for Morgana compared to control cells. The stars indicate signatures NF-κB related. **f** Immunoblotting of IκBα, Morgana and Vinculin in MDA-MB-231 cells EMPTY or shMORG1 and shMORG2 in combination or not with IκBα shRNA. **g** Luciferase assays of NF-κB activity in MDA-MB-231 cells described in **f**transfected with a NF-κB luciferase reporter or control vector. **h** Representative pictures of lungs of NSG mice after 4 weeks from the intravenous injection of MDA-MB-231 cells described in **f**. **i** Quantification of metastasis colonies in the lungs of mice described in **h** ($n = 6$ NSG mice per group). **j** Tumor weight 5 weeks after subcutaneous injection of cells described in **f** ($n = 3$ NSG mice per group). **k**, **l** Representative haematoxylin and eosin stained sections **k** and percentage of lung metastatic area **l**. Each data point represents one mouse ($n = 3$ NSG mice per group). Data are the results of three independent experiments. Bars in graphs represent standard errors (** $p < 0.01$; *** $p < 0.001$)

Notably, IκBα depletion completely reverted the metastatic impairment due to Morgana downregulation in MDA-MB-231 both in experimental (Fig. 3h, i) and spontaneous metastasis assays (Fig. 3j–l).

Morgana is an essential component of the IKK complex

To dissect the mechanism through which Morgana induces NF-κB activity, IκBα phopshorilation on serines 32 and 36 by the IKK complex was analysed in MDA-MB-231 and MCF7. We found that in MDA-MB-231 shMORG cells these residues were less phosphorylated compared to control cells (Fig. 4a). On the contrary, in MCF7, Morgana overexpression leads to a robust increase in IκBα phosphorylation on serines 32 and 36 compared to control cells (Fig. 4b). Immunoprecipitation experiments demonstrated that Morgana interacts with IκBα and the IKK complex in MDA-MB-231 (Fig. 4c) and Far Western experiment suggested that the interaction between Morgana and IκBα is direct (not shown). In gel filtration analysis of MDA-MB-231 total extracts, Morgana eluted together with IKKα and IKKβ in fractions around 1000–900 kDa (Fig. 4d). Co-immunoprecipitation experiments from these fractions demonstrated that Morgana binds to the mature IKK complex [72] (Fig. 4e). To evaluate the possibility that Morgana plays a function in the IKK complex assembly, we compared gel filtration experiments on total extracts from Morgana depleted and control cells. As shown in Fig. 4f, IKKα and IKKβ subunits eluted in the same high-molecular fractions, indicating that IKK complex assembly was not affected by Morgana silencing.

Morgana is essential for IκBα recruitment to the IKK complex, as assessed by IKKβ immunoprecipitation from MDA-MB-231 (Fig. 4g). In an *in vitro* IKKβ kinase assay the phosphorylation of a recombinant IκBα substrate was significantly impaired in Morgana downregulated cells compared to controls (Fig. 4h).

Figure 4

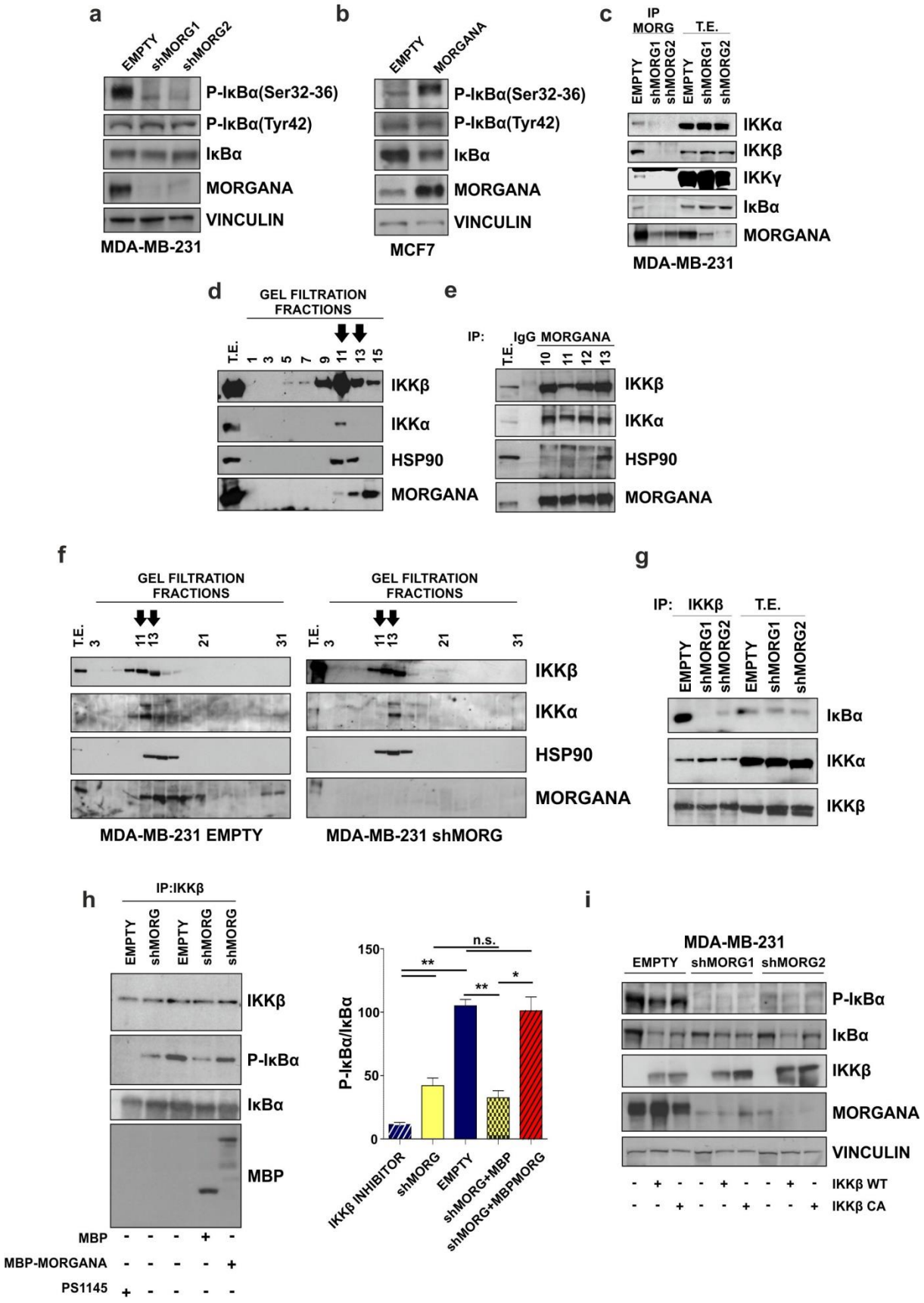
a
EMPTY
shMORG1
shMORG2
P-IκBα(Ser32-36)
P-IκBα(Tyr42)
IκBα
MORGANA
VINCULIN
MDA-MB-231
b
EMPTY
MORGANA
P-IκBα(Ser32-36)
P-IκBα(Tyr42)
IκBα
MORGANA
VINCULIN
MCF7
c
IP MORG
T.E.
EMPTY
shMORG1
shMORG2
EMPTY
shMORG1
shMORG2
IKKα
IKKβ
IKKγ
IκBα
MORGANA
MDA-MB-231
d
GEL FILTRATION FRACTIONS
T.E.
1
3
5
7
9
11
13
15
IKKβ
IKKα
HSP90
MORGANA
e
IP:
IgG
MORGANA
T.E.
10
11
12
13
IKKβ
IKKα
HSP90
MORGANA
f
GEL FILTRATION FRACTIONS
GEL FILTRATION FRACTIONS
T.E.
3
11
13
21
31
IKKβ
IKKα
HSP90
MORGANA
MDA-MB-231 EMPTY
MDA-MB-231 shMORG
g
IP:
IKKβ
T.E.
EMPTY
shMORG1
shMORG2
EMPTY
shMORG1
shMORG2
IκBα
IKKα
IKKβ
h
IP:IKKβ
EMPTY
shMORG
EMPTY
shMORG
shMORG
IKKβ
P-IκBα
IκBα
MBP
MBP - - - + -
MBP-MORGANA - - - - +
PS1145 + - - - -
P-IκBα/IκBα
150
100
50
0
n.s.
**
**
*
IKKβ INHIBITOR
shMORG
EMPTY
shMORG+MBP
shMORG+MBPMORG
i
MDA-MB-231
EMPTY
shMORG1
shMORG2
P-IκBα
IκBα
IKKβ
MORGANA
VINCULIN
- + - - + - - + - IKKβ WT
- - + - - + - - + IKKβ CA

Figure 4

Morgana is an essential component of the IKK complex in cancer cells. **a** Western blot of MDA-MB-231 infected with an empty vector (EMPTY) or two Morgana shRNAs (shMORG1, shMORG2). **b** Immunoblot of MCF7 infected with an empty vector (EMPTY) or overexpressing Morgana (MORGANA). **c** Immunoprecipitation of Morgana from MDA-MB-231 immunoblotted with IKKα, IKKβ, IKKγ, IκBα and Morgana. **d** Gel filtration analysis of the endogenous IKK complex purified from MDA-MB-231. The total protein extracts were fractionated on a Superose 6 gel filtration column. Each fraction was analyzed by Western blot. The arrows indicate the fractions in which Morgana and the IKK complex eluted together. **e** Immunoprecipitation of Morgana from selected fractions obtained by gel filtration immunochromatography of MDA-MB-231 immunoblotted with IKKα, IKKβ, HSP90 and Morgana. **f** Gel filtration analysis of total protein extracts from MDA-MB-231 shMORG1 (right) compared with control cells (left). Each fraction was analyzed by Western blot. The arrows indicate the fractions in which Morgana and the IKK complex eluted together. **g** Immunoprecipitation of IKKβ from MDA-MB-231 immunoblotted with IκBα, IKKα and IKKβ. **h** IKKβ was immunoprecipitated from MDA-MB-231 EMPTY and shMORG and subjected to an in vitro kinase assay with or without addiction of recombinant MBP-MORGANA or MBP as control. The IKKβ inhibitor, PS1145, was added to IKKβ immunoprecipitation from MDA-MB-231 EMPTY, as control. The graph shows the average intensity of the P-IκBα bands normalized to IκBα. **i** Immunoblotting of P-IκBα, IκBα, IKKβ, Morgana and Vinculin in MDA-MB-231 EMPTY or shMORG1 and shMORG2 transfected or not with IKKβ wild type (WT) or constitutively active (CA). Data are the results of three independent experiments. Bars in graphs represent standard errors (*$p < 0.05$; **$p < 0.01$)

However, the addition of an MBP-Morgana recombinant protein to the immunoprecipitate restored IκBα phosphorylation, while the recombinant MBP alone had no effect (Fig. 4h). This data indicates that Morgana is required per se to induce IκBα phosphorylation by IKKβ, without the need to recruit further elements to the complex. To understand whether Morgana activates IKKβ or mediates the recruitment of IκBα to the IKK complex we transfected MDA-MB-231 silenced for Morgana and control cells with a wild type or a constitutively active IKKβ. Our results showed that even in cell transfected with the constitutively active IKKβ, the IκBα phosphorylation is totally impaired when Morgana is silenced (Fig. 4i). Taken together, these results indicate a role for Morgana in mediating the binding of the IKK complex to its substrate

Morgana is co-expressed with NF-κB target genes

To evaluate the relevance of our molecular results in human breast cancer, we used a cohort of 152 patients from San Giovanni Battista Hospital (SGBH cohort) and bioinformatics analysis on TCGA datasets. Morgana expression significantly correlated with poor survival both in the TCGA dataset (Fig. 5a) and in the SGBH cohort of patients (Fig. 5b). Moreover, analyzing the TCGA protein array data in breast cancer specimens, we identified a significant correlation between Morgana expression and NF-κB activity, assessed by the analysis of p65 phosphorylation on serine 36 [73] (Fig. 5c). Moreover, GSEA analysis showed that several NF-κB gene signatures display positive correlation with Morgana expression in the breast cancer TCGA dataset (Fig. 5d, e). In particular, the expression of two well-known NF-κB target genes, IL-1β and MMP9, correlated with Morgana expression (Fig. 5f, g). Furthermore, analyzing by Real-time PCR 58 breast cancer samples from our SGBH patient cohort, we found a significant correlation between Morgana and MMP9 expression levels (Fig. 5h). In

accordance, on this cohort, the invasion grade was significantly higher in patients expressing high Morgana levels (Fig. 5i).

Figure 5

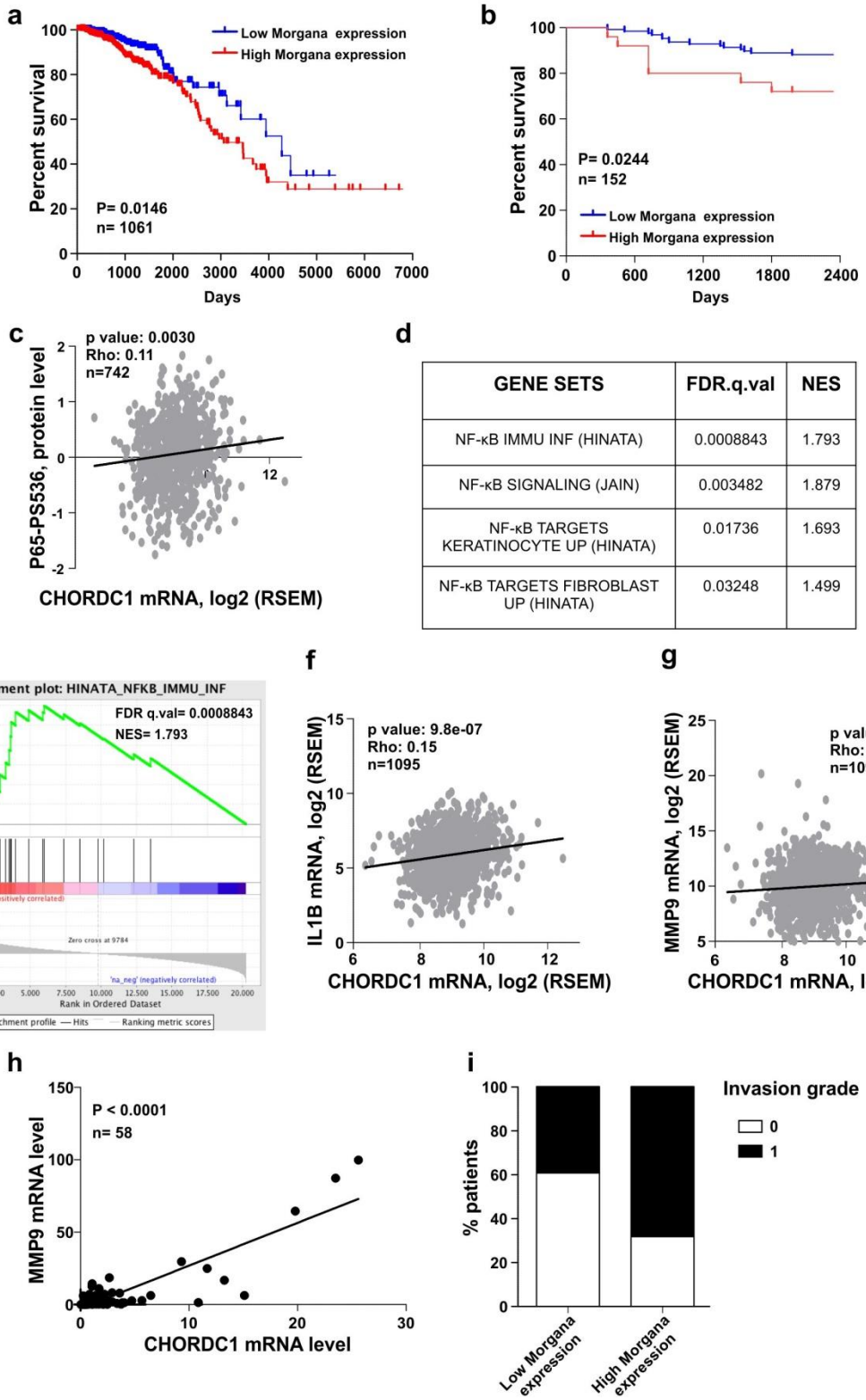

GENE SETS	FDR.q.val	NES
NF-κB IMMU INF (HINATA)	0.0008843	1.793
NF-κB SIGNALING (JAIN)	0.003482	1.879
NF-κB TARGETS KERATINOCYTE UP (HINATA)	0.01736	1.693
NF-κB TARGETS FIBROBLAST UP (HINATA)	0.03248	1.499

Figure 5

Morgana is co-expressed with NF-κB target genes in human breast cancers. **a** Morgana expression significantly correlated with poor survival in TCGA dataset ($P = 0.0146$, Mantel-Cox test). **b** Morgana expression significantly correlated with poor survival in San Giovanni Battista Hospital (SGBH) cohort of 152 patients ($P = 0.0244$, Mantel-Cox test). **c** Spearman correlation between CHORDC1 (Morgana coding gene) mRNA levels and the phosphorylation status of NF-κB p65 in Ser536 in 742 samples of TCGA dataset. **d** Table showing signature positively correlated with CHORDC1 mRNA levels generated by GSEA analysis of ranked NF-κB gene expression data in TCGA dataset. **e** Gene set enrichment analysis plot of the most CHORDC1-positively correlated NF-κB dataset. **f**, **g** Spearman correlation in mRNA levels between CHORDC1 and IL1B **f** and MMP9 **g** in TCGA data set ($n = 1095$). **h** Spearman correlation in mRNA levels between CHORDC1 and MMP9 in 58 patients from SGBH cohort. **i** Correlation between Morgana expression levels and vascular invasion grade indicated as 0 or 1 in 152 human breast cancer samples of SGBH cohort

Morgana modulates immune cell recruitment

Due to Morgana ability in modulating NF-κB and the role of its target genes in immune modulation, we used two transplantable models in syngeneic immunocompetent mice. We used respectively two mouse mammary carcinoma cells, 4T1 and E0771. The experiments on the two cell lines produced similar data and only 4T1 results will be shown in this manuscript. As in human breast cancer cells, Morgana downregulation in 4T1 (Fig. 6a), whereas not affecting proliferation *in vitro* (Fig. 6b), clearly impacted on IκBα phosphorylation (Fig. 6c) and NF-κB target gene transcription (Fig. 6d).

4T1 silenced for Morgana or control cells were injected subcutaneously in BALB/c syngeneic female mice. Differently from *in vitro* culture (Fig. 6b), 4T1 cancer cells silenced for Morgana grew significantly less in mice (Fig. 6e). Moreover, the ability of Morgana to regulate NF-κB activity was retained *in vivo*, since the transcription of different NF-κB target genes in the primary tumour was reduced when Morgana expression was downregulated (Fig. 6f). Cytofluorimetric analysis of disaggregated primary tumours (30 days from cell injection) indicated that Morgana depleted tumours recruited less neutrophils (Fig. 7a, b). Both primary tumour growth and neutrophil recruitment were totally rescued by IκBα silencing in 4T1 shMORG (Fig. 7a-d), demonstrating the causative role of NF-κB in these events. Analysis at an early time point (10 days from 4T1 injection), when tumour sizes were still comparable, confirmed that neutrophil recruitment in primary tumour depends on Morgana expression (Fig. 7e-g).

Even earlier (4 days from injection of 4T1), we noticed a significant increase in natural killer (NK) cells in Morgana downregulated tumours (Fig. 8a–c). No differences were found in other immune cells (Fig. 7a, f and 8b) and endothelial cells at all time points (not shown). NK cells are innate lymphoid cells playing a relevant role in cancer immune surveillance. Their cytotoxic activity is regulated by a number of activating and inhibitory signals triggered by cell surface receptors on the target cell [74].

Figure 6

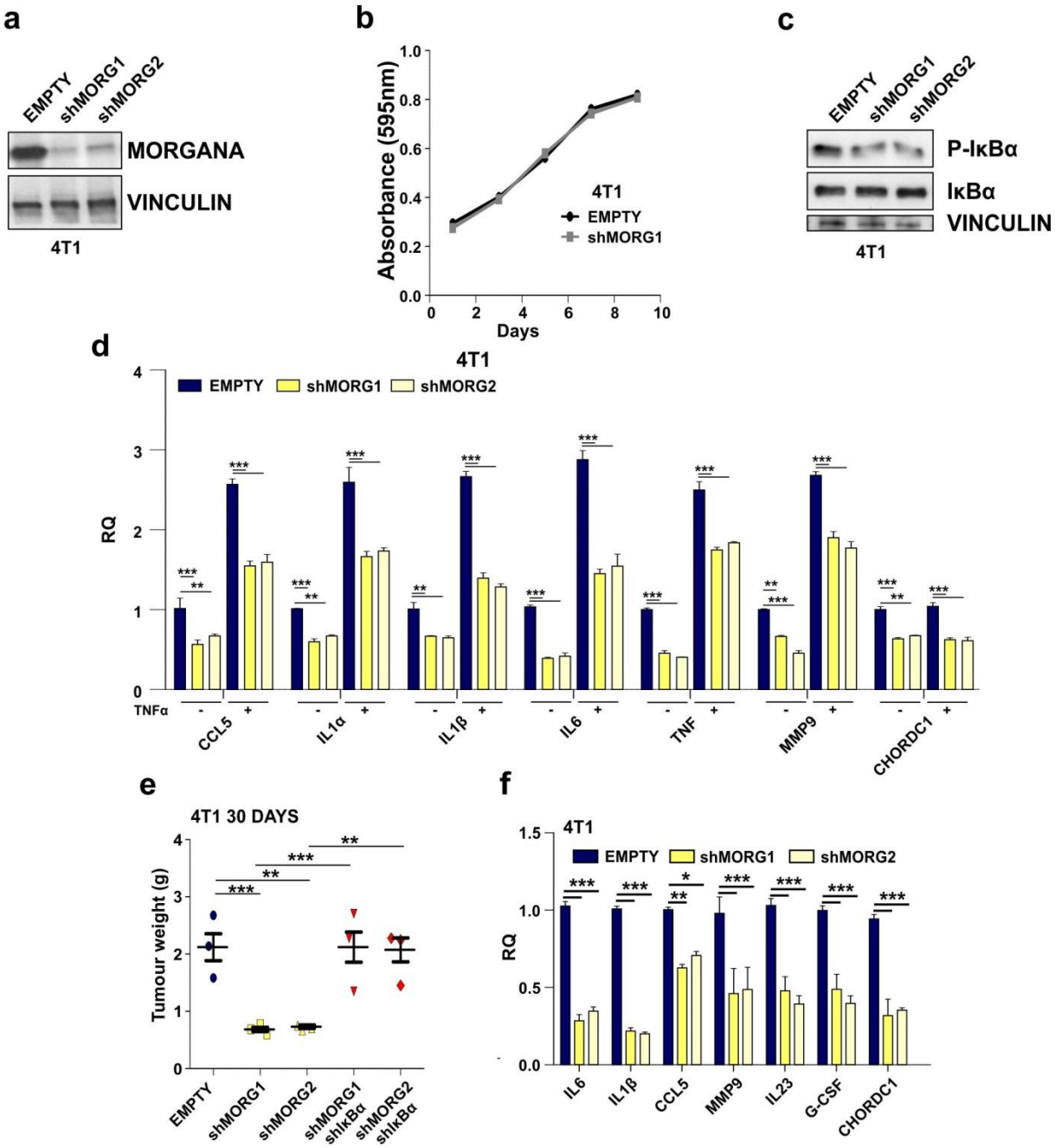

Figure 6

NF-κB activation is regulated by Morgana levels in mouse breast cancer cells. **a** Immunoblot of 4T1 infected with empty vector (EMPTY) or two different Morgana shRNAs (shMORG1 and shMORG2). **b** Growth curves of 4T1 EMPTY or shMORG1 and shMORG2. **c** Western blot analysis of P-IκBα, IκBα and Vinculin in 4T1 EMPTY or shMORG1 and shMORG2. **d** Gene expression analysis by Real-time PCR of NF-κB target genes in 4T1 EMPTY or shMORG1 and shMORG2 treated or not with 10nM TNFα for 4h. **e** Tumor weight 30 days after subcutaneous injection of 4T1 cells EMPTY or shMORG1 and shMORG2 infected or not with IκBα shRNA ($n = 3$ BALB/c mice per group). **f** Gene expression analysis by Real-time PCR of NF-κB target genes analyzed in primary tumours derived from 4T1 EMPTY or shMORG1 and shMORG2. Data are the results of three independent experiments. Bars in graphs represent standard errors (*p < 0,05; **p < 0.01; ***p < 0.001).

Figure 7

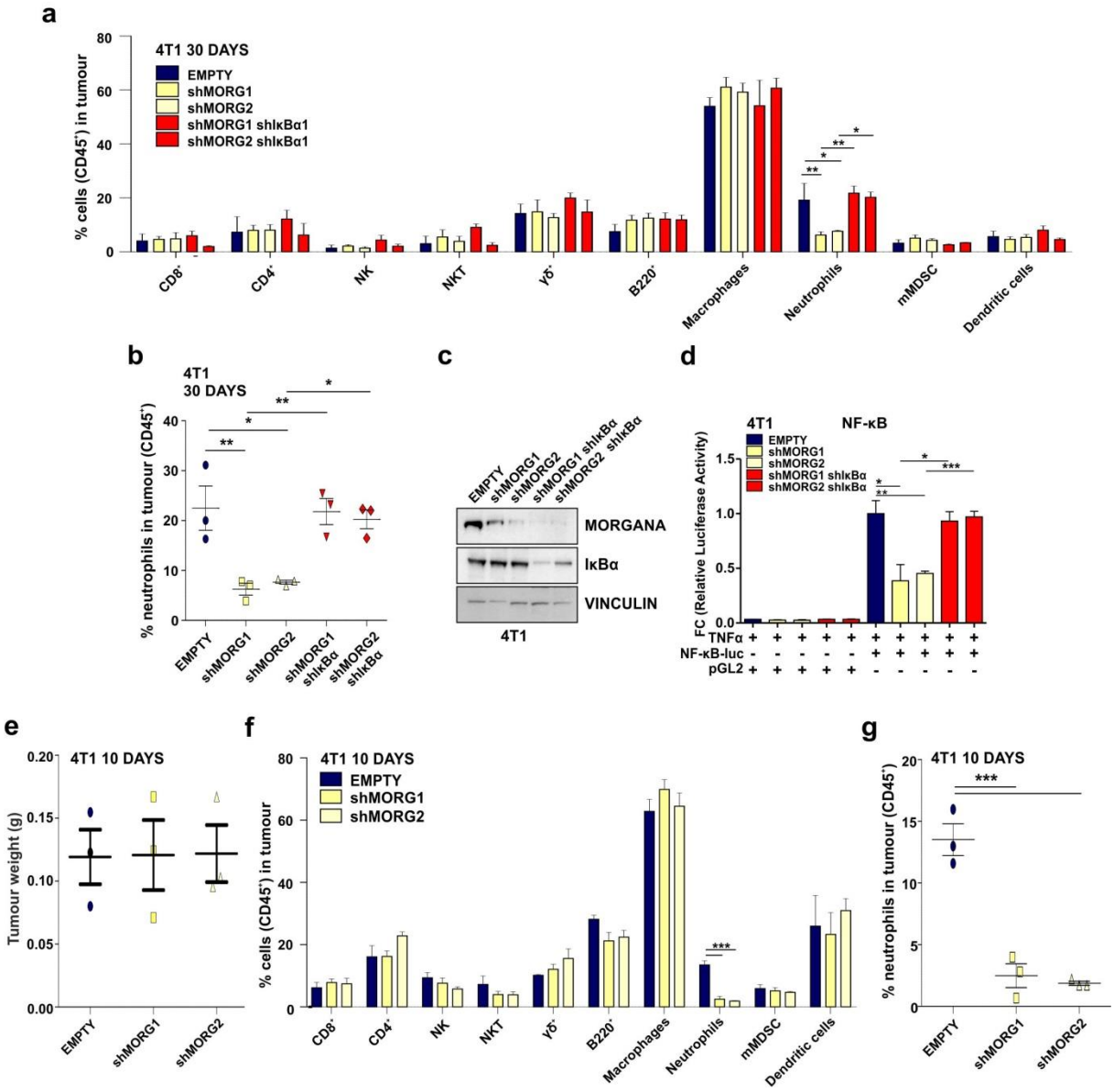

Figure 7

Morgana-NF-κB axis in breast cancer cells induces neutrophil recruitment in primary tumor. **a** Percentage of immune cells (gated on $CD45^+$ cells) detected in the primary tumor 30 days after injection of 4T1 described in **6e** ($n = 3$ BALB/c mice per group). **b** Percentage of neutrophils detected in the primary tumor of each mouse 30 days after injection of 4T1 cells described in **6e**. **c** Immunoblotting of Morgana, IκBα and Vinculin in 4T1 cells described in **6e**. **d** Luciferase assays of NF-κB activity in 4T1 cells described in **6e** transfected with a NF-κB luciferase reporter or control vector. **e** Tumor weight 10 days after subcutaneous injection of 4T1 cells EMPTY or shMORG1 and shMORG2 ($n = 3$ BALB/c mice per group). **f** Percentage of immune system cells (gated on $CD45^+$ cells) detected in the primary tumor 10 days after injection of 4T1 EMPTY or shMORG1 and shMORG2 ($n = 3$ BALB/c mice per group). **g** Percentage of neutrophils detected in the primary tumor of each mouse 10 days after injection of 4T1. Bars in graphs represent standard errors (*$p < 0.05$; **$p < 0.01$; ***$p < 0.001$)

Among others, the expression of MHC class I receptors on cancer cells potently inhibits NK activation. Accordingly, microarray and real time PCR analysis on MDA-MB-231 and 4T1 (Fig. 8d–e) highlighted a decrease in MHC class I receptors. Of note, MDA-MB-231 silenced for Morgana did not form tumour in nude mice, where, unlike in NSG mice, NK cells are present and functional [75] (Fig. 8f).

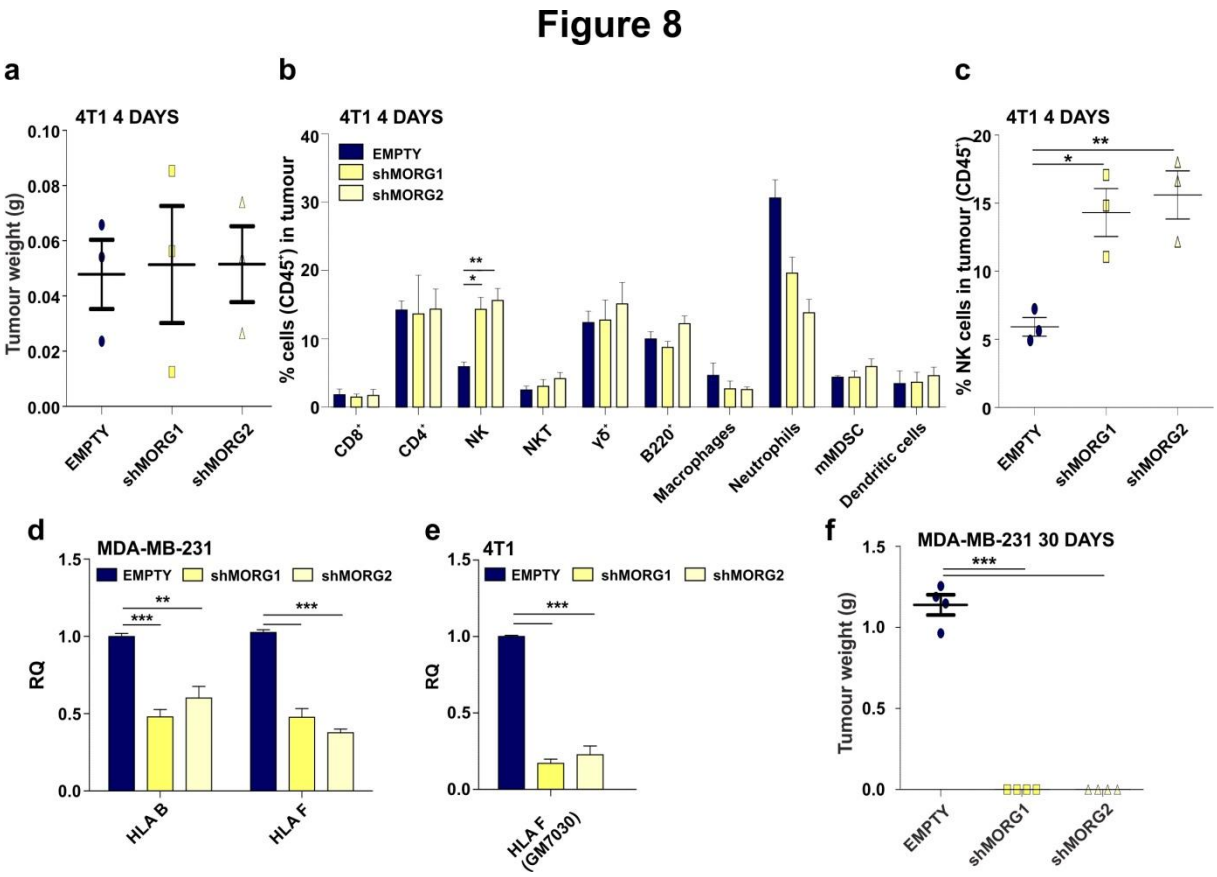

Figure 8

High Morgana levels in cancer cells induce NK cells recruitment at early phases of primary tumor formation. **a**, **b** Tumor weight **a** and percentage of immune cells (gated on $CD45^+$ cells) **b** 4 days after subcutaneous injection of 4T1 cells EMPTY or shMORG1 and shMORG2 ($n = 3$ BALB/c mice per group). **c** Percentage of natural killer (NK) cells detected in the primary tumor of each mouse 4 days after injection of 4T1. **d** Gene expression analysis by Real-time PCR of HLA-F and HLA-B in MDA-MB-231. **e** Gene expression analysis by Real-time PCR of GM7030 gene (mouse ortholog of HLA-F) in 4T1 EMPTY or shMORG1 and shMORG2. **f** Graph showing the tumor weight 30 days after injection of MDA-MB-231 EMPTY or shMORG1 and shMORG2 ($n = 4$ nude mice per group). Bars in graphs represent standard errors (*$p < 0.05$; **$p < 0.01$; ***$p < 0.001$)

Besides differences in primary tumour growth, we observed a dramatic impairment in spontaneous lung metastasis formation in syngeneic mice carrying Morgana downregulated tumours that it was rescued by IκBα silencing (Fig. 9a). Recently, it has been demonstrated

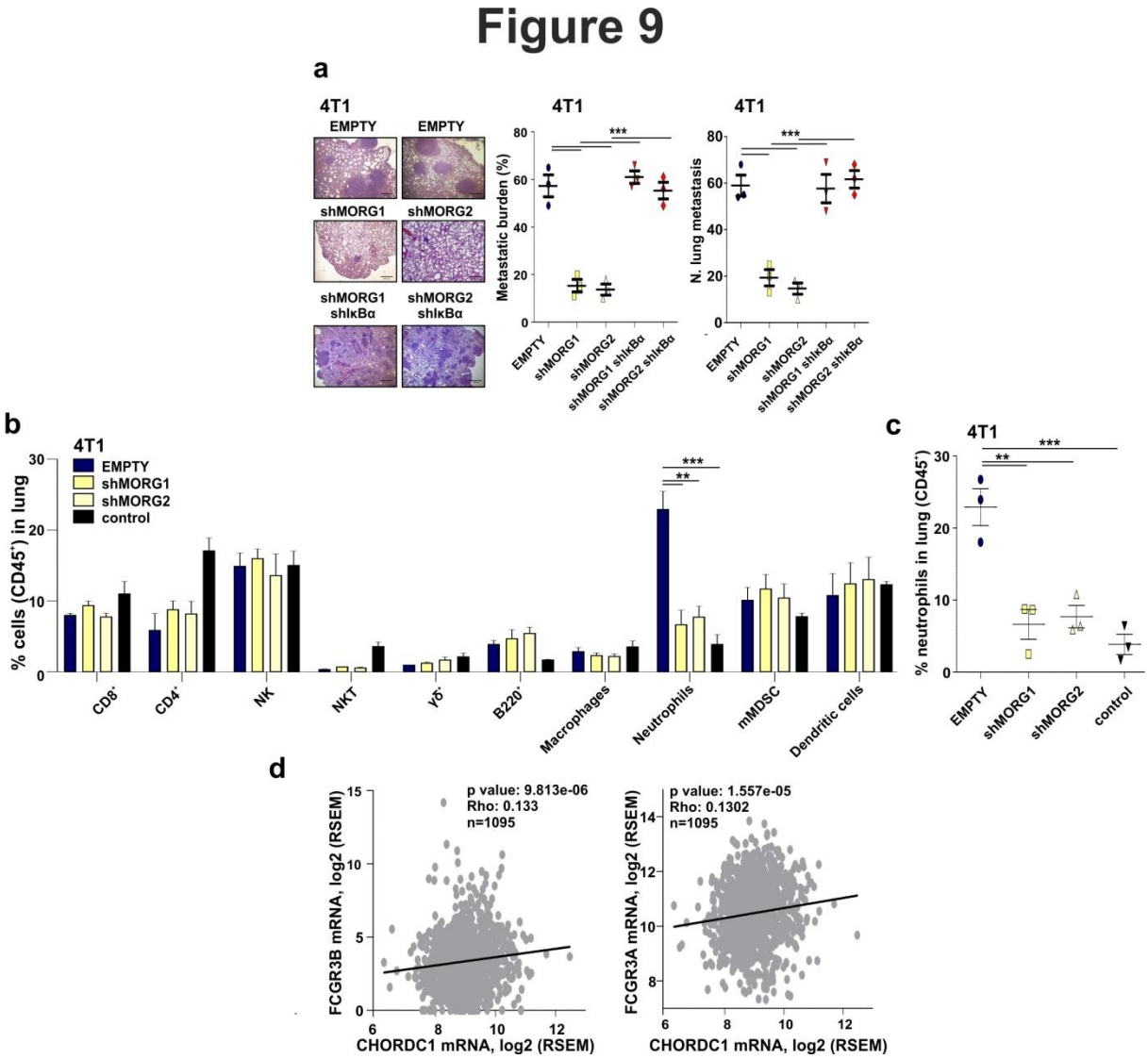

Figure 9

High Morgana levels in cancer cells induce neutrophil recruitment in the lung pre-metastatic niche. **a** Rapresentative haematoxylin and eosin stainings (left), quantification of lung metastatic area (middle) and number of lung metastases (right) of mice, 30 days after subcutaneous injection of 4T1 EMPTY or shMORG1 and shMORG2 infected or not with IκBα shRNA (n = 3 BALB/c or C57BL/6 mice per group). b Percentage of immune cells detected in lungs of mice, 10 days after injection of 4T1 EMTPY or shMORG1 and shMORG2 cells (n = 3 BALB/c mice per group). c Percentage of neutrophils recruited in the lungs of each mouse 10 days after injection of 4T1. d Spearman correlation in mRNA levels between CHORDC1 (Morgana coding gene) and neutrophils marker (FCGR3A and FCGR3B). Bars in graphs represent standard errors (**$p < 0.01$; ***$p < 0.001$).

that neutrophils, other than promoting tumour growth and progression [76], are crucial in preparing the breast cancer pre-metastatic niche in the lung [77, 78]. Very interestingly, neutrophil recruitment in mice carrying early stage tumours, when no differences in size were present, was heavily reduced in the lungs of mice injected with Morgana silenced cells (Fig.

9b, c). To demonstrate the relevance of Morgana expression in recruiting immune cells in human tumours, we performed a correlation between Morgana expression levels and genes typically expressed by neutrophils, lymphocytes and macrophages using the TCGA data set expression data. Morgana expression levels positively correlated with neutrophil markers FCGR3A (CD16) and FCGR3B (CD16b) (Fig. 9d), while no correlation was detected with lymphocyte (MS4A1 coding for CD20 and CD19) and macrophage markers (CD68 and CD14) (not shown), indicating a specific role of the Morgana/NF-κB axis in neutrophil recruitment also in human cancers.

Overall these results indicate that Morgana expression in tumour cells is necessary to produce cancer cell immune escape and neutrophil recruitment in primary tumour and pre-metastatic niche (Fig. 10).

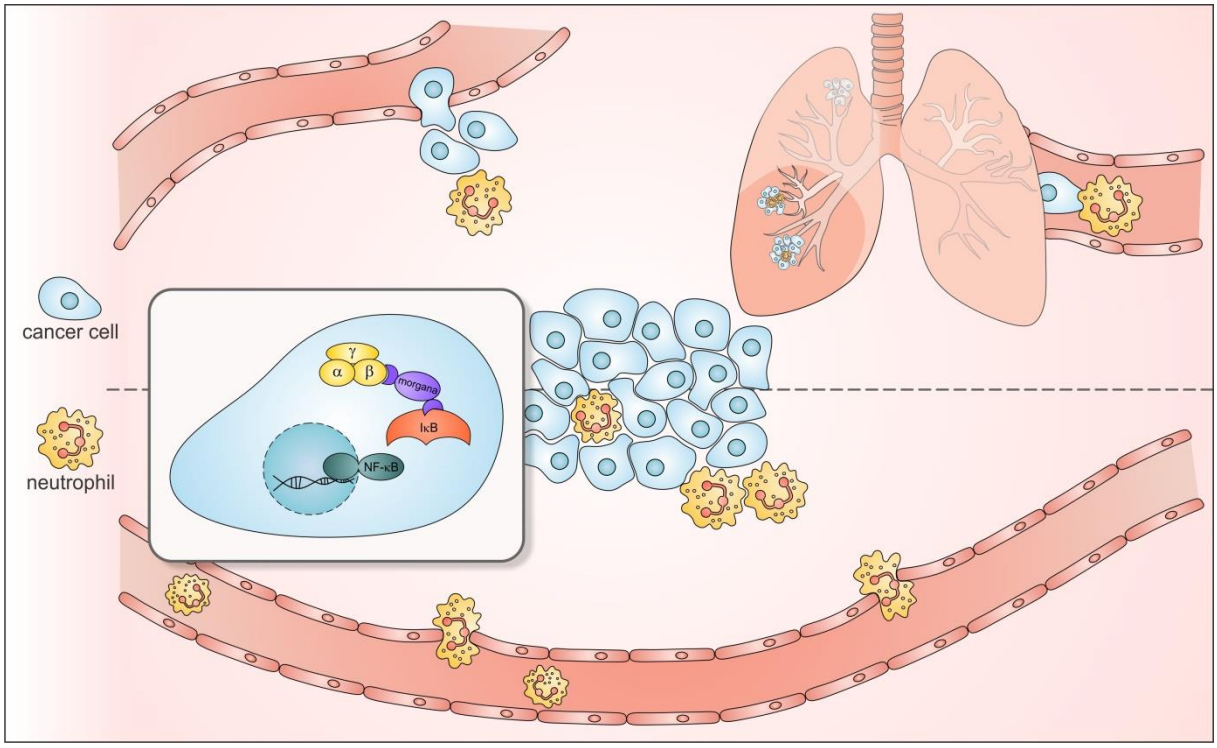

Figure 10

Schematic model based on our study showing an essential role for Morgana in connecting IKK complex and its substrate IκBα. The consequent activation of NF-κB in the tumor induces the production of several cytokines able to modulate the recruitment of cells of the immune system promoting metastatic spreading of tumor cells. *Fusella F, Seclì L, Brancaccio M. Escaping NK cells and recruiting neutrophils: How Morgana/NF-κB signaling promotes metastasis. Mol Cell Oncol. 2018*

eMorgana induces migration in TNBC cells through TLR2 and TLR4

Triple negative breast cancer cells secrete Morgana unconventionally

The secreted proteins from cancer cells are believed to play a deterministic role in cancer progression and therefore may be the key to find novel therapeutic targets and biomarkers for many cancers [79]. Analysing cancer cell secretomes using the Human Cancer Secretome Database [80], we found that many types of tumour cells secrete Morgana (Fig. 11a). As shown in Figure 11b, we validated this data, analysing the conditioned medium (CM) of breast cancer cells. Morgana as the chaperones HSP90 and HSP70, is secreted by breast cancer cell lines and not by MCF-10, a model of normal breast epithelial cell line. We believe that Morgana is free in the conditioned medium since we were able to see by Western blotting and to immunoprecipitate it without the use of any detergent.

We know that Morgana binds to HSP90 in the cytoplasm [9] and given that both these proteins are present in the CM of cancer cells, we investigated the possibility that they interact also in the extracellular milieu. Also in this case we performed all the experiments in parallel in MDA-MB-231 and BT-549 but only the results on the first cell line will be shown. By immunoprecipitating Morgana from the CM of these cell lines we were able to co-immunoprecipitate HSP90, demonstrating that Morgana and HSP90 interact also in the extracellular milieu (Fig. 11c). However, their association is not required for their secretion, in fact Morgana is secreted also if HSP90 is downregulated and viceversa (Fig. 11c, d).

Proteins secreted through the conventional pathway are transported from the endoplasmic reticulum to the Golgi and then to the plasma membrane where they are released into the extracellular space. However, many proteins lack the canonical signal peptide needed to enter the endoplasmic reticulum and reach the extracellular milieu using unconventional pathways, including direct translocation across plasma membranes, secretory lysosome, autolysosomes, amphisomes, autophagosomes and exosomes [53]. Using SecretomeP [81], a method for the prediction of unconventional protein secretion, we found that Morgana is predicted to be secreted by an uncanonical pathway (0,582: proteins addressed to non-canonical pathways get a score above 0,5). Accordingly, blocking the ER-Golgi transport using Brefeldin A, we were able to impair the secretion of proteins known to use the canonical pathway, like MMP9, laminin and fibronectin, but not of Morgana and other HSPs like HSP90 and HSP70 (Fig. 11e). Moreover, as shown in Fig. 11f Morgana was present in exosomes prepared from MDA-MB-231 CM, together with HSP90 and HSP70. We can conclude that Morgana is present in the CM both as free protein and included in exosomes but it is important to understand if

other unconventional pathways are involved, since uncanonical secreted proteins, like Il-1β, FGF2 and HMGB1 reach the medium using different mechanisms [53].

Figure 11

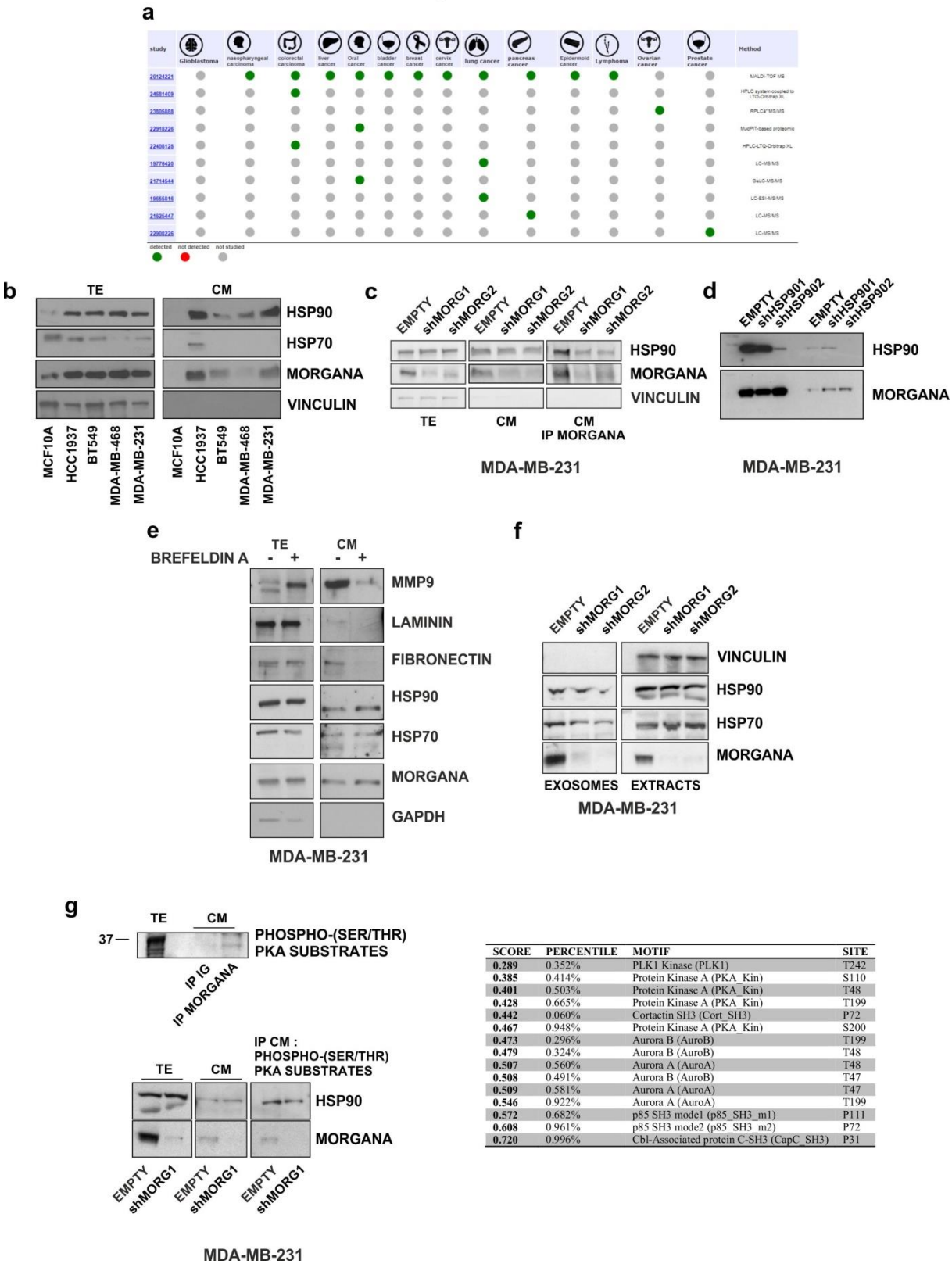

SCORE	PERCENTILE	MOTIF	SITE
0.289	0.352%	PLK1 Kinase (PLK1)	T242
0.385	0.414%	Protein Kinase A (PKA_Kin)	S110
0.401	0.503%	Protein Kinase A (PKA_Kin)	T48
0.428	0.665%	Protein Kinase A (PKA_Kin)	T199
0.442	0.060%	Cortactin SH3 (Cort_SH3)	P72
0.467	0.948%	Protein Kinase A (PKA_Kin)	S200
0.473	0.296%	Aurora B (AuroB)	T199
0.479	0.324%	Aurora B (AuroB)	T48
0.507	0.560%	Aurora A (AuroA)	T48
0.508	0.491%	Aurora B (AuroB)	T47
0.509	0.581%	Aurora A (AuroA)	T47
0.546	0.922%	Aurora A (AuroA)	T199
0.572	0.682%	p85 SH3 mode1 (p85_SH3_m1)	P111
0.608	0.961%	p85 SH3 mode2 (p85_SH3_m2)	P72
0.720	0.996%	Cbl-Associated protein C-SH3 (CapC_SH3)	P31

Figure 11

Triple negative breast cancer cells secrete Morgana unconventionally. **a** Analysis of Morgana presence in cancer cell secretomes using the Human Cancer Secretome Database. **b** Total protein extracts (TE) and conditioned mediums (CM) of MCF10, HCC-1937, BT549, MDA-MB-468 and MDA-MB-231 cells were analyzed with western blotting to evaluate the different expression of Morgana, HSP90 and HSP70. **c** Immunoprecipitation of Morgana from conditioned medium (CM) of MDA-MB-231 EMPTY and depleted for Morgana, shMORG1 and shMORG2, analysed for HSP90 presence. **d** Total extracts (TE) and conditioned mediums (CM) of MDA-MB-231 EMPTY and depleted for HSP90, shHSP901 and shHSP902, analysed for Morgana presence. **e** Total extracts (TE) and conditioned mediums (CM) of MDA-MB-231 treated with the inhibitor of classical proteins secretion, Brefeldin A (10 µg ml-1, 5 h). MMP9, LAMININ and FIBRONECTIN reached the medium passing through the ER-Golgi system. HSP90, HSP70 and Morgana used unconventional mechanisms. GAPDH is a cytoplasmic protein **f** Western blot of exosomes and total extracts (TE) of MDA-MB-231 EMPTY and shMORG1 and shMORG2 blotted for HSP90, HSP70 and Morgana. **g** On the left. Immunoprecipitation of Morgana from the conditioned medium (CM) of MDA-MB-231 blotted with Phospho-(Ser/Thr) PKA substrates antibody. Viceversa, immunoprecipitation from the conditioned medium (CM) of MDA-MB-231 EMPTY and shMORG of Phospho-(Ser/Thr) PKA substrates, blotted with HSP90 and Morgana antibodies. On the right. Analysis performed on Morgana structure using Scansite 3.0 to predict the presence of motifs potentially phosphorylated by PKA.

It is known that Protein Kinase A (PKA) mediated phosphorylation of HSP90 at Thr-90 and this modification is essential for its secretion [67]. By immunoprecipitating Morgana in the CM of MDA-MB-231, we were able to recognise a specific signal at 37kDa (Morgana molecular weight) using the PKA phospho-substrates antibody, able to recognize phosphorylated Ser/Thr residues presented on PKA substrates. And viceversa, immunoprecipitating PKA phospho-substrates from the CM of MDA-MB-231 cells, we found co-immunoprecipitated both HSP90 and Morgana, suggesting that eMorgana is phosphorylated by PKA. This result was supported by the analysis performed on Scansite 3.0 [82], that highlighted the presence of motifs potentially phosphorylated by PKA (Fig. 11g). Further analysis are needed to deepen the results and to understand how PKA actively phosphorylates Morgana in cancer cells.

Extracellular Morgana (eMorgana) induces migration in breast cancer cells through TLR2 and TLR4

Once HSP reach the medium, promote cancer progression and metastasis formation, inducing cell migration [61, 64]. To investigate the migratory role of eMorgana, we produced a recombinant protein fused to Maltose Binding Protein (MBP). It is known that the Lipopolysaccharide (LPS), also known as endotoxin, the major component of *E.coli* outer membrane, induces migration per se in mammalian cells and activates the immune system. We used ClearColi® BL21(DE3) cells [83], genetically modified *E.coli* strain that doesn't trigger the endotoxin signal, to avoid confounding results due to LPS contamination of our recombinant proteins. Performing a wound healing assay on MDA-MB-231 shMORG cells and control cells, we found that Morgana downregulation causes an impairment in the migratory ability of this cancer cell line. However, the addition of the recombinant MBP-Morgana, and not MBP, in the medium, was able to totally rescue the migratory impairment of shMORG cells (Fig. 12a). Study performed with deletion mutants (only CHORD domains

or only CS domain) clearly indicated that only the full length Morgana is able to restore migration in MDA-MB-231 cells when added in the medium (not shown).

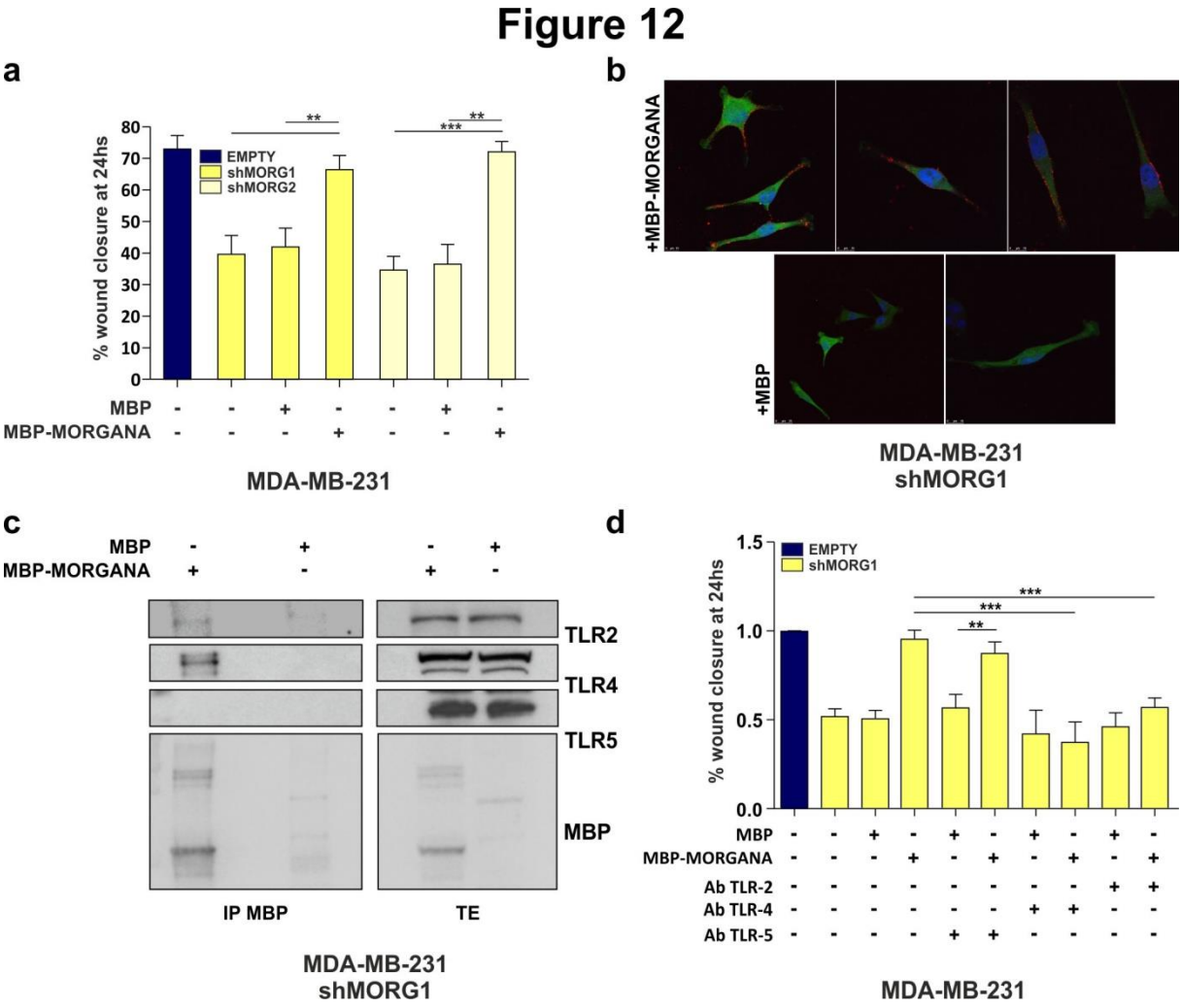

Figure 12

Extracellular Morgana (eMorgana) induces migration in breast cancer cells through TLR2 and TLR4. **a** Quantitative representation of the wound healing assay. MDA-MB-231 EMPTY and depleted for Morgana, shMORG1 and shMORG2, were wounded and images captured immediately and after 24 h. MDA-MB-231 shMORG1 and shMORG2 were treated with 0,1 μM of MBP or MBP-MORGANA. Column is the average of three independent experiments. Within a single experiment, each condition was test in duplicate. **b** Immunofluorescence of MDA-MB-231 shMORG1 cells treated with MBP or MBP-MORGANA. Cells without permeabilization, were stained with MBP antibody (red) and DAPI nuclear marker (blue). **c** shMORG1 MDA-MB-231 cells were treated with MBP or MBP-MORGANA (0,1 μM, 1 h, 4 °C), crosslinked with DTSSP (1 mM, 2 h, 4 °C) and lysed with CHAPS buffer. After MBP immunoprecipitation, total extracts (TE) were analyzed for the presence of TLR2, 4 and 5 by western blotting. **d** MDA-MB-231 (treated with 0,1 μM of MBP or MBP-MORGANA alone or in combination with a monoclonal antibody against TLR2 (30ng/ml), TLR4 (100μM), TLR5 (100μM)) were wounded and images captured immediately and 24 h after wounding. Column is the average of three independent experiments. Within a single experiment, each condition was test in duplicate. Bars in graphs represent standard errors (**$p < 0.01$; ***$p < 0.001$).

To understand how eMorgana induces migration in breast cancer cells, we asked if Morgana is able to exert its function binding membrane receptors. We performed an immunofluorescence confocal analysis of MDA-MB-231 shMORG cells, treated with the recombinant proteins MBP or MBP-MORGANA. We stained treated cells with an anti-MBP antibody without permeabilization of the plasma membrane to highlight the possibility that

eMorgana exerts its pro-migratory functions by binding surface receptors. As shown, only cells treated with MBP-MORGANA highlighted the presence of a punctuated staining on the membrane (Fig. 12b).

As said before, DAMPs and in particular HSPs can act on cancer cells via pattern recognition receptors (PRRs) such as TLR2 and TLR4, inducing cell motility and metastasis formation [84].

To investigate if eMorgana binds to TLRs, we treated in parallel MDA-MB-231 shMORG cells with MBP or MBP-MORGANA and after reinforcing the binding to the cell membrane with an impermeable crosslinker, we immunoprecipitated MBP from the total cell lysates. TLR2 and TLR4, but not TLR5 were present in the immunoprecipitation of cells treated with MBP-MORGANA compared to cells treated with MBP alone, suggesting a possible involvement of these receptors in eMorgana function (Fig. 12c). In order to support these data, we performed a wound healing assay in which cells interfered for Morgana were treated with MBP or MBP-MORGANA in combination with a neutralizing antibody against TLR2, TLR4 or TLR5. After 24 hours we observed that only the antibodies against TLR2 and TLR4 were able to block MBP-MORGANA activity in inducing migration, while TLR5 antibody did not affect eMorgana function.

Materials and Methods

Cell culture

The human MDA-MB-231, MDA-MB-468 and the murine 4T1, B16, LLC cell lines were cultured in DMEM medium (Thermo Fisher Scientific) with 10% FBS (Euroclone) and 1% Penicillin Streptomycin (Thermo Fisher Scientific). Human BT549 cells were cultured in RPMI medium (Thermo Fisher Scientific) with 0.023 IU ml^{-1} insulin (Sigma Aldrich), 10% FBS (Euroclone) and Penicillin Streptomycin (Thermo Fisher Scientific). Human MCF10A cells were maintained in DMEM/F12 Ham's medium 1:1, 5% horse serum (Thermo Fisher Scientific), insulin (10 µg ml^{-1}, Sigma Aldrich), hydrocortisone (0.5 µg ml^{-1}, Sigma Aldrich), epidermal growth factor (EGF 20 ng ml^{-1}, Sigma Aldrich) and Penicillin Streptomycin (Thermo Fisher Scientific). Human HeLa, HCC1937 and murine E0771 cells were cultured in RPMI medium (Thermo Fisher Scientific) with 10% FBS (Euroclone) and 1% Penicillin Streptomycin (Thermo Fisher Scientific). Murine NIH-3T3 cells were maintained in DMEM medium (Thermo Fisher Scientific) with 10% FCS (Thermo Fisher Scientific) and 1% Penicillin Streptomycin (Thermo Fisher Scientific).

Morgana knockdown in MDA-MB-231, BT549, HeLa, HEK293, 4T1, and E0771 was performed by infecting cells with pGIPZ lentiviral particles expressing two different Morgana shRNAs, together with the TurboGFP (Open Biosystems). BT549, MCF10A, MCF7, and NIH-3T3 overexpressing Morgana were obtained using a pLVX lentiviral vector coding for mouse Morgana fused to a myc tag. MMP9 overexpression was obtained infecting BT549 and MDA-MB-231 with PLX304-MMP9. HSP90 and CDC37 downregulation in MDA-MB-231 was performed by infecting cells with pLKO lentiviral particles expressing two different HSP90 or CDC37 shRNAs. IκBα silencing was obtained using pGIPZ lentiviral particles for MDA-MB-231 and pLKO viral particles for 4T1 and E0771.

Plasmids and shRNA

The following shRNAs were obtained from Open Biosystems: human CHORDC1 shRNAs V2LHS_24674 and V2LHS_24745; human IkBα shRNA V3LHS_410687, mouse CHORDC1 shRNAs V2THS_24746 and V2THS_24674. The following shRNAs were obtained from Sigma: human HSP90 shRNAs NM_007355.2-232s1c1 and NM_007355.2-2239s21c1; human CDC37 shRNAs NM_007065.3–819s1c1 and NM_007065.3-818s1c1,

mouse IkBα shRNA NM_010907.2-235s21c1. IKK-2 WT (Addgene plasmid #11103) and IKK-2 S177E S181E (Addgene plasmid #11105) were gifts from Anjana Rao. p1242 3x-KB-L was a gift from Bill Sugden (Addgene plasmid #26699) and 3xAP1pGL3 (3xAP-1 in pGL3-basic) was a gift from Alexander Dent (Addgene plasmid #40342).

Antibodies and reagents

Western blotting and immunoprecipitations were performed using the following primary homemade antibody: P1/PP0 using GST-Morgana fusion protein as an antigen [6] and MBP using MBP protein as antigen. Other commercially antibodies were used: Vinculin (Sigma, SAB4200080, 1:5000), CHORDC1 (Sigma, HPA041040, 1:1000), MMP9 (Abcam, ab76003, 1:1000), MMP2 (Santa Cruz, 8835, 1:500), HSP90 (Santa Cruz, 13119, 1:1000), HSP70 (Thermo Fisher Scientific, MA3-008, 1:1000). IkBα Ser32-36 (Santa Cruz, 8404, 1:500), P-IkBα Tyr42 (Abcam, ab24783, 1:1000), IkBα (Cell Signaling, 4814, 1:1000), IKKα (Cell Signaling, 11930, 1:1000), IKKα (Cell Signaling, 2682, 1:100 for co-immunoprecipitation experiments), IKKβ (Cell Signaling, 8943, 1:1000), IKKγ (Santa Cruz, 8032, 1:500), αTubulin (Sigma, T5168, 1:8000), MBP (Cell Signaling, 2396, 1:1000), TNF-R1 (Santa Cruz, 8436, 1:500), TAK-1 (Santa Cruz, 166562, 1:500), p-AKT (Cell Signaling, 9271, 1:1000), AKT (Cell Signaling, 4691, 1:1000), CDC37 (Santa Cruz, 5617, 1:500), P-IKKα/β (Cell Signaling, 2697, 1:1000), Phospho-PKA Substrate (Cell Signaling, 9624, 1:1000), TLR2 (Blocking: Biolegend, 121802, 30 ng ml^{-1}; Western blotting: Abcam, 108998, 1:1000), TLR4 (Blocking: Abcam, 8376, 100µM; Western blotting: Santa Cruz, 293072), TLR5 (Blocking: InvivoGen, maba2-htlr5, 100µM; Western blotting: Abcam, 13876, 1:1000).

TNFα (300-01A and 315-01A) was purchased from Peprotech, the IKKβ inhibitor PS1145 (P6624), ROCK inhibitor Y27632 (Y0503), the PTEN inhibitor VO-OHpic (V8639), and the AKT inhibitor GSK69093 (SML0428) were from Sigma. BEZ235 (S1009) was purchased from Selleckchem.

Lentiviral transduction

Virus containing supernatants were collected 48 h after co-transfection of pCMV-VSV-G, pCMV Δ8.2 and the shRNA- or ORF-containing vector into HEK293T cells, and then added to the target cells. Cells were then selected with 10 µg ml^{-1} puromycin [9].

Anchorage-independent growth assay

Soft agar colony formation assay on MDA-MB-231 was performed by resuspending cells in complete DMEM (Gibco-BRL) containing 0.3% low gelling agarose (Sigma-Aldrich) and seeding cells in triplicate into 6 well plates containing a 2 ml layer of solidified 0.6% agar (Sigma-Aldrich). After 2 weeks colonies were stained with nitroblue tetrazolium (Sigma-Aldrich), photographed with Zeiss microscopy (Carl Zeiss) and colonies were counted using the ImageJ Software.

Cell proliferation assay

MDA-MB-231, BT549, 4T1, and E0771 cell growth curves were generated by plating 1×10^4 cells and staining cells with 0.1% crystal violet at the indicated times. After staining, wells were destained with 20% acetic acid and the absorbance of crystal violet solution was measured at 595 nm.

Gelatin zymography

For gelatin zymography, conditioned media and total protein extracts were collected from confluent MDA-MB-231 cells maintained in serum-free media for 24 h. Samples were subjected to electrophoresis using 10% denaturing polyacrylamide gels containing 0.1% gelatin. Following electrophoresis, gel were renatured with 25% Triton in dH2O and incubated at 37 °C for 16 h in a buffer composed of 500 mM Tris–HCl, pH 7.8; 2 M NaCl and 50 mM CaCl2. Then gels were stained with 0,5% Coomassie blue in 5% methanol, and 10% acetic acid in dH_2O and destained with 10% methanol, 5% acetic acid in dH_2O. The bands on the gels were quantified using the ImageJ software.

Immunoprecipitation and western blot analysis

MDA-MB-231 or BT549 were lysed with lysis buffer (25 mM Tris–HCl pH 8, 1 mM MgCl2, 10 mM NaF, 1 mM PMSF, 1 mM Na3VO4 and cocktail protease inhibitors (Roche)). After the lysis, cells were centrifuged at 1677 g for 5 min and then supernatants were ultra-centrifuged at 256365 g for 1 h. 500 ng of total protein extracts was incubated overnight at 4 °C with 5 μg of the selected antibody, then protein G-coated Sepharose was added for 45 min (GE Healthcare). Beads were washed 10 times in lysis buffer and resuspended in Laemmli buffer. For Western blot analysis, cells were lysed in Tris-buffered saline with 1% Triton X-100, plus phosphatase and protease inhibitors. Total protein extracts (30–50 μg) were analyzed by Western blotting and detected by the chemiluminescent reagent LiteAblot (Euroclone). Band intensities were quantified using Quantity One software (Bio-Rad).

Receptor immunoprecipitation

MDA-MB-231 or BT549 were treated with MBP or MBP-MORGANA (0,1 μM, 1h, 4 °C) and crosslinked with DTSSP (1 mM, 2 h, 4 °C). After blocking the reaction with 35 mM Tris–HCl pH 7,5 at 4 °C for 15 min cells were lysed with 0,7% CHAPS buffer (25 mM Hepes pH 7,6, 120 mM NaCl, 2 mM EDTA in H_2O) plus protease inhibitors. Cells were centrifuged at 13000 rpm for 15 min and after supernatants were incubated overnight at 4 °C with 5 μg of MBP antibody. Then protein G-coated Sepharose was added for 60 min (GE Healthcare). Beads were washed 5 times in lysis buffer and resuspended in Laemmli buffer and DTT (50 mM).

Conditioned medium

$2x10^6$ cells were plated in a 100 mm dish and allowed to settle for 24 hours. Cells were then re-fed with 10 ml serum free medium and 1% MEM Non-Essential Amino Acids Solution (Thermo Fisher Scientific 100X) and incubated for 48 hours at 37 °C. Conditioned medium was collected and concentrated at 2000 g by centrifugation with Vivaspin 20 centrifugal concentrator MWCO10,000 Da (Sigma-Aldrich) up to 1 ml. For immunoprecipitation 1 ml of conditioned medium was incubated with 5 μg of interest antibody or control IgG. For Brefelin A (Sigma-Aldrich) treatment, the compound was added to the medium at 10 μg ml^{-1} for 5 h, then conditioned medium and total extract of MDA-MB-231 and BT549 were analysed by Western blotting.

Exosomes

$7x10^6$ cells were plated in a 150 mm dish and allowed to settle for 24 hours. Cells were then re-fed with 10 ml serum free medium and incubated for 48 hours at 37 °C. Conditioned medium was collected and centrifugated at 2000 g for 20 min at 4 °C. Then the medium was collected, putted in a new tube and centrifugated at 10000 g for 30 min at 4 °C. The medium was collected again, passed through 200 μm filter, putted in a new tube and centrifugated at 100000 g for 70 min at 4 °C. The medium was aspirated and PBS was added and another centrifugation of 100000 g for 70 min at 4 °C was performed. The medium was aspirated and the pellet was lysed directly in SDS buffer.

Transwell invasion assay

Invasion assays for MDA-MB-231 and BT549 were performed using BioCoat TM Matrigel Invasion Chambers with 8.0 µm pore size membrane (Becton Dickinson). Cells were previously starved for 24 h. Then, cells (75×10^3) were plated in the top chamber in medium without serum or growth factors, lower chambers were filled with complete growth media. After 24 h, the migrated cells present on the lower side of the membrane were fixed in 2.5% glutaraldehyde and stained with 0.1% crystal violet. For MDA-MB-231 transwell were photographed using an Olympus IX70 microscope. Invasion was evaluated by measuring the area occupied by migrated cells using the ImageJ software. For BT549 the invasion absorbance was measured after destaining of crystal violet with 20% acetic acid and the absorbance of crystal violet solution was measured at 595 nm.

Expression plasmids, recombinant protein production and LPS purification

To obtain recombinant full-length CHP-1 (aa 1–331) the coding sequences was inserted into pGEX-5X-3 plasmid (GE Healthcare). DNA fragments were generated by PCR using specific primers containing EcoRI and SmaI recognition sites and previously described pMALc2-Chp-1 as a template [6]. Protein production was carried out in 500 mL cultures of Escherichia coli BL21 ClearColi® [83]. Expression was induced with 1 mM IPTG at OD 600 0,7 and bacteria were cultured at 37°C for 4 h. Bacterial cultures were centrifugated at 3000 rpm for 30 min at 4°C and pellets were resuspended in Column Buffer (Tris-HCL 20 mM, NaCl 200 mM, EDTA 1 mM, ZnCl2 1 µM). Following freezing to induce partial bacteria membrane lysis, bacteria were sonicated with eight pulse of 15 seconds at 38% of amplitude and centrifugated at 13000 rpm for 30 minutes at 4°C. Supernatants (crude extracts) were incubated with amylose resin (New England Biolabs) overnight at 4°C and then loaded together in column. After washing, the fusion protein was eluted with a solution of Column Buffer and 10 mM maltose. Finally proteins were dialyzed against PBS.

Wound healing assay

$1{,}5x10^6$ MDA-MB-231 and BT549 cells were culture in 6-well plates. When 90% confluent, cells were starved 24 hours. Then, a wound was scratched in the center of the cell monolayer by a sterile plastic pipette tip. The debris were removed by washing with PBS and a solution of serum free medium and 1% MEM Non-Essential Amino Acids Solution (Thermo Fisher Scientific 100X) was placed in each well with either the vehicle control PBS, 0,1 µM recombinant MBP protein or 0,1 µM recombinant MBP-MORGANA protein, in combination or not with the neutralizing antibody against TLR2 (30 ng ml^{-1}), TLR4 (100 µM) or TLR5

(100 µM). The condition was used for the treatments with blocking antibody against Morgana (15 µg ml^{-1} when not specified). The image of the wound was captured at time 0 and after 24 hours at Zeiss microscopy (Carl Zeiss). The percentage of wound closure was calculated using Axio Vision programme.

Immunofluorescence

GFP shMORG cells ($30x10^3$) were cultured in 24-well plates. After 24 h were treated with MBP or MBP-MORGANA (0,1 µM) in serum free medium for 24 h. Cells were fixed and saturated. A primary antibody against MBP (1 h RT) was used to stain recombinant proteins on the cell membrane without permeabilization. Secondary antibody was added and Dapi staining was performed. Glasses were analysed with Z-stack using the confocal and 2 photon microscopes (Leica).

In vivo tumour and metastasis assays

Experiments were carried out in accordance with the ethical guidelines of the European Communities Council Directive (2010/63/EU). Experimental approval was obtained from the Italian Health Ministry. Experimental metastasis assay and in vivo rescue experiment with IκBα shRNA were performed by injecting 5×10^5 MDA-MB-231 cells (in PBS) into the tail vein of 7-weeks-old female immunodeficient NSG mice (Charles River Laboratories). Mice were dissected 4 weeks later and macrometastases were counted at Nikon SMZ1000 stereomicroscope. Spontaneous metastases were evaluated in 7-weeks-old female immunodeficient NSG mice injected with 1×10^6 MDA-MB-231 cells (in PBS) and dissected 5 weeks later. Macrometastases were counted at Nikon SMZ1000 stereomicroscope. 1×10^5 4T1 cells in 100 µl of PBS (mixed with Matrigel at 1:1 ratio) were injected subcutaneously in 6 weeks old female syngeneic BALB/c mice. After 4, 10, or 30 days mice were killed and the tumours were removed and weighed. 2×10^5 E0771 cells in 100 µl of PBS (mixed with Matrigel at 1:1 ratio) were injected subcutaneously in 6 weeks old female syngeneic C57BL/6 mice. After 6, 14 or 30 days mice were killed and the tumours were removed and weighed. For all metastasis studies, organs were formalin fixed and paraffin embedded, sectioned and haematoxylin and eosin (H&E) stained. Micrometastases were evaluated on specimens, with an Olympus BH2 microscope, on at least three different sections. Metastatic burden was evaluated as percentage of lung metastatic area using Metamorph Software (Universal Imaging Corporation), averaging at least six fields per sample. Experiments were performed in blind. 6 weeks old female immunocompromised nude mice were injected subcutaneously

with 1×10^6 MDA-MB-231 or BT549 cells and after 30 days mice were killed and the tumours, if present, were removed and weighed.

RNA isolation and Real-time PCR

Total RNA from cells or tumours was isolated using Trizol Reagent (Thermo Fisher Scientific), following the manufacturer's recommendations. RNA was reverse transcribed by using Applied Biosystem high capacity cDNA reverse transcription kit. Gene expression analysis was performed using TaqMan Gene Expression Assays (Applied Biosystems) on an ABI Prism 7900HT sequence detection system (Applied Biosystems). We used 18S (Thermo Fisher) as the endogenous control throughout all experimental analysis. Analysis was performed using the $\Delta-\Delta$Ct method to determine fold changes. We used gene-specific primers and the Universal Probe Library System (Roche Applied Sciences). Cells were treated or not with TNF-α 10 nM 4 h before RNA extraction.

Luciferase reporter assay

Plasmids for the Luciferase Assay were purchased from Addgene: p1242-3x-KB-L, containing 3 NF-kappaB binding sites upstream of the Firefly Luciferase gene and 3xAP1pGL3, containing 3 AP-1 binding sites upstream of the Firefly Luciferase gene. For the Luciferase Assay 8×10^4 cells were plated on a 24-well plate. After 24 h, cells were co-transfected using Lipofectamine 2000 (Invitrogen) with 150 ng of pRL-TK Vector (PROMEGA) containing the Renilla luciferase construct, used as a normalizer and internal control, and with 650 ng of reporter vector (p1242-3x-KB-L or 3xAP1pGL3), or with empty vector pGL2 or pGL3, respectively (Promega). After 24 h trasfection cells were treated with TNF-α 10 nM and after 24 h Dual-Luciferase Reporter Assay were performed by Glomax instrument (Promega). Results are calculated as fold changes and shown as means of Firefly Luciferase activity normalized on Renilla luciferase activity.

IKKβ kinase assay

IKKβ activity was detected by performing a cold kinase assay. MDA-MB-231 cells were lysed in IP buffer (Hepes 50 mM pH 7.6, NaCl 150 mM, EDTA 1 mM, 0.1% NP40, 10% glycerol, protease and phosphatase inhibitors), followed by centrifugation at 45346×g for 15 min. IKKβ was immunoprecipitated from an equal amount of protein extracts and protein G beads were resuspended in kinase buffer (20 mM Hepes pH 7.6, 20 mM MgCl2, 10 mM NaF, 0.1 mM Na3VO4, 5% glycerol, 1 mM DTT, Roche protease inhibitors cocktail and

1 mM PMSF). Then, we added ATP (10 μM) and 1 μg of IKBα substrate (Abcam) and 1 μg of MBP (Maltose Binding Protein) or 1 μg of MBP-Morgana or IKKβ inhibitor PS1145 20 μM to a volume of 25 μl at 30°C for 10 min. Reactions were stopped by adding an equal volume of 2× Laemmli buffer, followed by incubation at95 °C for 10 min. Kinase activity was detected by Western blotting using P-IκBα and IκBα antibodies.

Far western

In total 1 μg of recombinant prey proteins was run on SDS–PAGE and transferred to nitrocellulose membrane. Proteins were denatured by incubating the membrane in the AC buffer (100 mM NaCl, 20 mM Tris pH 7.6, 0.5 mM EDTA, 10% glycerol, 0.1% Tween 20, 2% skim milk powder and 1 mM DTT) containing 6 M guanidine-HCl for 30 min at RT. Then with the AC buffer containing 3 M guanidine-HCl for 30 min at RT. This is followed by incubation with the AC buffer containing 0.1 M and no guanidine-HCl at 4°C for 30 min and 1 h, respectively. After blocking with 5% milk for 1 h RT, the membrane was incubated with the bait recombinant protein MBP-MORGANA overnight at 4°C. Chemiluminescent detection was performed after the membrane incubation with the primary (1 h at RT) and the secondary antibody (1 h RT).

Flow cytometry

Single-cell suspensions from murine tumours and lungs were prepared by mechanical and enzymatic disruption in PBS with 1 mg ml^{-1} collagenase P (Roche) for 1 h. Cells in suspension were filtered through a 40 μm cell strainer and centrifuged for 5 min at 120 g. After lysis of red blood cells, FcR were blocked with an anti-CD16/CD32 antibody (Becton Dickinson) and cells were stained with the indicated fluorochrome-conjugated antibodies and Propidium Iodide (Sigma) to analyze viable cells. Lymphoid cell detection, samples were stained with anti-CD45, CD3, CD4, CD8, CD49b, B220, and γδ TCR antibodies, and % were calculated gating on the $CD45^+$ population, while for myeloid and endothelial cell analysis samples were stained with anti-CD45, CD11b, F4/80, Ly6C, Ly6G, CD206, and CD31 and reported as percentage of myeloid cells on the $CD45^+$ population or of $CD31^+$ endothelial cells on the $CD45^-$ population. Dendritic cell (DC) subsets were stained with anti-CD45, CD11b, CD11c, CD24, CD64, IA/IE+, and Ly6G antibodies. The percentage of neutrophils was calculated as $CD45^+$, $CD11b^+$, $F4/80^-$, $Ly6C^+$, and $Ly6G^+$ cells. The percentage of natural killer cells (NK) was calculated as $CD45^+$, $CD3^-$ and $CD49b^+$, while percentage of NKT was calculated as $CD45^+$, $CD3^+$, and $CD49b^+$. The percentage of T lymphocytes was

calculated as $CD45^+$, $CD3^+$, $CD8^+$. For each analysis, a total of at least 20000 $CD45^+$ living cells were analyzed. Flow cytometric analyzes were carried out on a BD FACSVerse using BD FACSSuite Software (Becton Dickinson).

Gel filtration chromatography

Gel filtration chromatography was performed on a Superose-6 10/300 GL column (GE Healthcare) using an AKTA purifier system (GE Healthcare). Protein extract was loaded onto the column and separated in gel filtration buffer (25 mM Tris–HCl pH 8.0, 1 mM MgCl2, 10% glycerol), at a flow rate of 0,3 ml min^{-1} and 0,5 ml fractions were collected. The molecular mass standards (GE Healthcare) used to calibrate the column were blue dextran (2000 kDa), thyroglobulin (669 kDa), ferritin (440 kDa), catalase (240 kDa) and aldolase (158 kDa). The fractions were directly analyzed by Western blotting after concentration using Nanosep 3 K or immunoprecipitated with anti-Morgana antibody and analyzed by Western blotting.

Microarray

Total RNA was extracted using Trizol and Absolute RNA miRNA kit (Agilent) following manufacturer's instructions. In total 1 µg of total RNA was amplified with ammino-allyl message amp II kit (Ambion) and labeled with Cy3 (GE-Heathcare), using the indirect labeling protocol. a total of 200 ng of labeled RNA were hybridized on Agilent SurePrint G3 Human Gene Expression 8×60 K glass arrays. The glass slide was scanned using an Agilent scanner and images were analyzed using Agilent Feature Extraction Software (version 10.7.3.1). Raw data were then processed using the Bioconductor package Limma (Linear models for microarray analysis). Differentially expressed transcripts were retrieved applying 0.01 as adjusted p-value cut-off and +1 or −1 as logFC cut-off for up or downregulation, respectively.

RNA preparation from tissue array specimens

This study was conducted in compliance with the ethical regulatory requirements for the handling of biological specimens after appropriate informed consent and Institutional Review Board approval. The follow up study was performed on 152 samples of the tissue array previously described [69]. RNA from 58 human specimens was prepared using MasterPure complete DNA and RNA purification kit (Epicentre).

Statistical significance

For sample size calculation one tail Fisher test was used. Each experiment was repeated three times or more. The data are presented as means ± SEM. For statistical analyzes, significance was tested using a two-tailed Student's t test or, when required, one or two-way ANOVA with Bonferroni's correction. A minimum value of $p < 0.05$ was considered to be statistically significant. Statistical analyzes were performed using GraphPad Prism 4. The Mantel-Cox test was used in Kaplan-Meier survival curves.

Statistics for spearman correlation analysis

Spearman correlation analyzes were performed using the R language, Rstudio suite and 'cor.test' function, method = 'spearman'. P values were adjusted for multiple testing with 'p.adjust' function, method = 'fdr'. Gene expression data (HiseqV2) and protein RPPA-RBN data of TCGA BRCA, samples, version: 2015-02-24, were downloaded from UCSC Cancer Genome Browser65,66,67,68 (http://genome-cancer.ucsc.edu). Gene expression data and metadata of 54 breast cancer cell lines38 were downloaded from XENA Cancer Browser (xenabrowser.net).

GSEA analysis

Gene Set Enrichment Analysis was performed by running the GSEAPreranked tool from command line (gsea2-2.2.0.jar, with the following parameters: -mode Max_probe,-norm meandiv,-nperm 1000, -rnd_seed timestamp,-set_max 500 and-set_min 15). The list's ranking metric was calculated on the Spearman's Rho correlation coefficient between CHORDC1 expression levels and all the genes present in the analyzed cohort (for what concern TCGA BRCA, 20530 genes in 1095 primary tumour samples cohort; while for Heiser's samples 18632 genes in 54 breast cancer cell lines). The gene sets used in the analysis, were downloaded (on May 16, 2016) from the Broad Institute GSEA website (http://software.broadinstitute.org/gsea/index.jsp), MSigDB database v5.2.

Discussion

In this work we identify Morgana as an important player in carcinogenesis. We previously described that Morgana, inhibiting ROCK II, destabilizes PTEN, leading to the maintenance of PI3K/AKT survival pathway [69] and this molecular mechanism leads TNBC cells to acquire resistance to chemotherapy. In this study we identified an additional molecular mechanism by which Morgana robustly sustain cancer progression. Indeed, we showed that Morgana interacts with the mature IKK complex, and although it is not required for the complex formation, it is essential for the recruitment of IκBα and for its phosphorylation. Consequently, Morgana potently regulates NF-κB transcriptional activity and target gene expression in different breast cancer cell lines. Interestingly we found that this also happens in non-tumourigenic and primary cells (not shown), indicating that Morgana may act as a general regulator of NF-κB activity. However, further work is needed to understand the relevance of Morgana in other cellular contexts and in response to different NF-κB activating stimuli. Importantly, Morgana silencing, by inhibiting NF-κB pathway, was able to almost completely block cancer cell metastasis. Bioinformatics studies on TCGA breast cancer dataset, coupled with analysis on a cohort of 152 breast cancer patients, confirmed a correlation between Morgana expression levels, NF-κB activity and poor survival in human breast cancer patients. NF-κB activation in cancer cells, mediating the secretion of a number of cytokines and soluble factors, impacts on the tumour microenvironment and establish of a vicious circle capable of maintaining a chronic inflammatory state and fuel cancer growth and progression [85, 86]. Indeed cancer cells engage essential relationship with normal cells inducing their pathological activation by secreting a plethora of cytokines. In turn, inflammatory cells and activated fibroblasts support cancer growth and progression producing cytokines and soluble factors. Moreover, cancer cells must evade immune surveillance, through a number of mechanisms such as targeting the regulatory T cell function or inducing immune system tolerance or ignorance. Our data indicate that Morgana signaling plays a fundamental role both in inducing immune escape and in recruiting ancillary cells in the tumour microenvironment. Indeed, high Morgana expression level in cancer cells inhibits the recruitment of NK cells during the very early phases of cancer formation, while it induces neutrophil accumulation in subsequent steps. The fact that human breast cancer cells silenced for Morgana grow in NSG mice but not in nude mice, where NK cells are present and functional [75], further supports a role for Morgana in cancer cell immune escape through NK

inhibition. Considering the innovative therapeutic approaches to activate NK anti-tumour activity, Morgana overexpression may represent an important biomarker to direct clinical intervention towards the blockage of NK inhibitory receptors [86]. On the other hand, the pivotal role of neutrophils in cancer onset and progression has been recently recognized [76]. Cancer-derived chemokines induce neutrophil proliferation and egression from the bone marrow and their polarization toward a pro-tumour phenotype, able to promote primary tumour growth and spread. NF-κB activation, through IκBα silencing, in cancer cells downregulated for Morgana totally rescues primary tumour growth and neutrophil recruitment, demonstrating a causal role of Morgana/NF-κB signaling in these events. Moreover, besides being recruited to the primary tumour, neutrophils accumulate in the pre-metastatic niche and drive metastatic initiation [44, 77, 78, 87]. Morgana downregulation in breast cancer cells, by quenching NF-κB signaling, inhibits neutrophil recruitment and the formation of the pre-metastatic niche in the lung, preventing metastasis formation.

In addition, we recently found that Morgana is actively secreted in the extracellular milieu of TNBC cell lines. HSPs secretion is a prerogative of stressed and cancer cells and this notion supports the fact that MCF10, a normal breast cell line, is not able to secrete HSP90, HSP70 as well as Morgana. Moreover, it is important to note, that Morgana secretion is an active mechanism not due to cell death. Indeed we were not able to find in the medium cytoplasmic proteins like Vinculin, described to be release only after necrotic events. Normally, the stimuli that promote HSPs secretion include inflammation, hypoxic environment and heat shock however further studies are needed to dissect the molecular mechanism that regulates HSPs secretion. If on the one hand it is clear that HSPs use unconventional pathways, on the other hand it is unclear if a single alternative pathway is responsible for their secretion or if different mechanisms are activated simultaneously. Once in the extracellular milieu, HSPs can exert their function in an autocrine fashion on malignant cells, tuning different aspects of cancer progression. For example, extracellular HSP90 plays a remarkably powerful role in stimulating cancer cell migration, invasion and metastasis formation [65]. In line with these data, we demonstrated that eMorgana has a pro-migratory effect on cancer cells acting through TLR2 and TLR4. We believe that this binding and activity is independent from HSP90 but other experiments are needed to confirm this idea. We know that both Morgana and HSP90 secretion happens independently from each other and preliminary experiments suggest that HSP90 is not necessary for the binding of eMorgana to TLR2 and 4. This could be consistent with the results of Thuringer and colleagues that demonstrated that HSP90 is

able to bind specifically to TLR4 and not to TLR2 in glioblastoma cancer cells [88]. The use of a specific inhibitor against eHSP90 would be important to definitively understand if eMorgana does not require eHSP90 for its extracellular function. . In literature there are some examples of extracellular HSP90 selective inhibitors like the mAb 4C5, that is described to impairs breast and melanoma cancer cell migration, invasion and metastasis [89] as well as the small molecule DMAG-N-oxide that significantly retarded melanoma cells to invade and colonize the lungs [90]. Unfortunately these compounds are not yet commercially available and this aspect remains open to further analysis. Toll-like receptors, as said previously, are considered key sensors of pathogen invasion and are expressed on cells of the immune system but they were also found on cancer cells, where they may influence tumour initiation and progression [84]. Indeed, some agonists and antagonists of TLRs have been utilized for anti-cancer immunotherapy in clinical trials [91, 92]. In cancer cells the response triggered by TLRs activation depends on the type of receptor involved and on the specific ligand. Normally TLRs activation promotes cell growth, migration, invasion and resistance to apoptosis. If in many cases these effects are cell autonomous, often they are due to the involvement of the tumour microenvironment. Indeed pro-inflammatory molecules released by cancer cells after the activation of TLRs can in turn modulate the nearest cells, from fibroblasts to endothelial and immune cells, favouring the progression of the disease and its immune evasion [93]. Between TLRs, TLR2 and TLR4 are known to be receptors for eHSPs on cancer cells but also on immune cells. Indeed the interaction between eHSP and TLRs were first identified in immune cells and then extended to cancer. Extracellular HSPs, are known to functions as cytokines leading to the activation of NF-κB and MAPKs in immune cells. In particular, they have been described to stimulate the proliferation, migration, and cytolytic activity of NK cells, the activation of monocyte and macrophages and the T cell activation with the consequent production of IFN-γ [94]. All these data are consistent with the fact that eHSPs in cancer can elicit their effect also through paracrine mechanisms, on the immune cells present in the tumour microenvironment. Depending on the eHSP, the stimulus on different immune cell types can be immnoactivatory or immunesuppressive and can respectively lead to a better or a worst outcome in cancer progression. In this view it will be essential to identify the potential role of eMorgana on immune cells in inflammation and cancer. Although many aspects still remain open, the extracellular Morgana has the potentiality to became an attractive biomarker in the serum of breast cancer patients and could represent a new targetable protein for reducing migration and metastasis formation, the most aggressive aspect of TNBC.

References

1. Shirasu, K. *et al.* A novel class of eukaryotic zinc-binding proteins is required for disease resistance signaling in barley and development in C. elegans. *Cell* **99**, 355-366 (1999).
2. Garcia-Ranea, J.A., Mirey, G., Camonis, J. & Valencia, A. p23 and HSP20/alpha-crystallin proteins define a conserved sequence domain present in other eukaryotic protein families. *FEBS letters* **529**, 162-167 (2002).
3. Brancaccio, M. *et al.* Chp-1 and melusin, two CHORD containing proteins in vertebrates. *FEBS letters* **551**, 47-52 (2003).
4. Ferretti, R. *et al.* Morgana and melusin: two fairies chaperoning signal transduction. *Cell Cycle* **10**, 3678-3683 (2011).
5. Brancaccio, M. *et al.* Melusin is a new muscle-specific interactor for beta(1) integrin cytoplasmic domain. *The Journal of biological chemistry* **274**, 29282-29288 (1999).
6. Ferretti, R. *et al.* Morgana/chp-1, a ROCK inhibitor involved in centrosome duplication and tumorigenesis. *Developmental cell* **18**, 486-495 (2010).
7. Hahn, J.S. Regulation of Nod1 by Hsp90 chaperone complex. *FEBS letters* **579**, 4513-4519 (2005).
8. Hong, T.J. *et al.* Dynamic nucleotide-dependent interactions of cysteine- and histidine-rich domain (CHORD)-containing Hsp90 cochaperones Chp-1 and melusin with cochaperones PP5 and Sgt1. *The Journal of biological chemistry* **288**, 215-222 (2013).
9. Michowski, W. *et al.* Morgana/CHP-1 is a novel chaperone able to protect cells from stress. *Biochimica et biophysica acta* **1803**, 1043-1049 (2010).
10. Sbroggio, M. *et al.* The mammalian CHORD-containing protein melusin is a stress response protein interacting with Hsp90 and Sgt1. *FEBS letters* **582**, 1788-1794 (2008).
11. Takahashi, A., Casais, C., Ichimura, K. & Shirasu, K. HSP90 interacts with RAR1 and SGT1 and is essential for RPS2-mediated disease resistance in Arabidopsis. *Proceedings of the National Academy of Sciences of the United States of America* **100**, 11777-11782 (2003).
12. Wu, J., Luo, S., Jiang, H. & Li, H. Mammalian CHORD-containing protein 1 is a novel heat shock protein 90-interacting protein. *FEBS letters* **579**, 421-426 (2005).
13. Li, J., Soroka, J. & Buchner, J. The Hsp90 chaperone machinery: conformational dynamics and regulation by co-chaperones. *Biochimica et biophysica acta* **1823**, 624-635 (2012).
14. Bose, S., Weikl, T., Bugl, H. & Buchner, J. Chaperone function of Hsp90-associated proteins. *Science* **274**, 1715-1717 (1996).
15. Hartl, F.U., Bracher, A. & Hayer-Hartl, M. Molecular chaperones in protein folding and proteostasis. *Nature* **475**, 324-332 (2011).
16. Saibil, H. Chaperone machines for protein folding, unfolding and disaggregation. *Nature reviews. Molecular cell biology* **14**, 630-642 (2013).
17. Rappa, F. *et al.* HSP-molecular chaperones in cancer biogenesis and tumor therapy: an overview. *Anticancer research* **32**, 5139-5150 (2012).
18. Ciocca, D.R. & Calderwood, S.K. Heat shock proteins in cancer: diagnostic, prognostic, predictive, and treatment implications. *Cell stress & chaperones* **10**, 86-103 (2005).
19. Wu, J. *et al.* Heat Shock Proteins and Cancer. *Trends Pharmacol Sci* **38**, 226-256 (2017).
20. Xu, W. & Neckers, L. Targeting the molecular chaperone heat shock protein 90 provides a multifaceted effect on diverse cell signaling pathways of cancer cells. *Clin Cancer Res* **13**, 1625-1629 (2007).
21. Mahalingam, D. *et al.* Targeting HSP90 for cancer therapy. *British journal of cancer* **100**, 1523-1529 (2009).
22. Trepel, J., Mollapour, M., Giaccone, G. & Neckers, L. Targeting the dynamic HSP90 complex in cancer. *Nat Rev Cancer* **10**, 537-549 (2010).

23. Srivastava, P. Roles of heat-shock proteins in innate and adaptive immunity. *Nature reviews. Immunology* **2**, 185-194 (2002).
24. Chovatiya, R. & Medzhitov, R. Stress, inflammation, and defense of homeostasis. *Mol Cell* **54**, 281-288 (2014).
25. Goldstein, M.G. & Li, Z. Heat-shock proteins in infection-mediated inflammation-induced tumorigenesis. *Journal of hematology & oncology* **2**, 5 (2009).
26. Knowlton, A.A. NFkappaB, heat shock proteins, HSF-1, and inflammation. *Cardiovascular research* **69**, 7-8 (2006).
27. Moseley, P.L. Heat shock proteins and the inflammatory response. *Annals of the New York Academy of Sciences* **856**, 206-213 (1998).
28. Quail, D.F. & Joyce, J.A. Microenvironmental regulation of tumor progression and metastasis. *Nature medicine* **19**, 1423-1437 (2013).
29. Dvorak, H.F. Tumors: wounds that do not heal. Similarities between tumor stroma generation and wound healing. *The New England journal of medicine* **315**, 1650-1659 (1986).
30. Crusz, S.M. & Balkwill, F.R. Inflammation and cancer: advances and new agents. *Nature Reviews Clinical Oncology* **12**, 584 (2015).
31. Grivennikov, S.I., Greten, F.R. & Karin, M. Immunity, inflammation, and cancer. *Cell* **140**, 883-899 (2010).
32. de Visser, K.E., Eichten, A. & Coussens, L.M. Paradoxical roles of the immune system during cancer development. *Nat Rev Cancer* **6**, 24-37 (2006).
33. Fusella, F. *et al.* The IKK/NF-kappaB signaling pathway requires Morgana to drive breast cancer metastasis. *Nature communications* **8**, 1636 (2017).
34. Siegel, R.L., Miller, K.D. & Jemal, A. Cancer statistics, 2018. *CA: a cancer journal for clinicians* **68**, 7-30 (2018).
35. Dawson, S.J., Provenzano, E. & Caldas, C. Triple negative breast cancers: clinical and prognostic implications. *European journal of cancer* **45 Suppl 1**, 27-40 (2009).
36. Hammond, M.E. *et al.* American Society of Clinical Oncology/College Of American Pathologists guideline recommendations for immunohistochemical testing of estrogen and progesterone receptors in breast cancer. *Journal of clinical oncology : official journal of the American Society of Clinical Oncology* **28**, 2784-2795 (2010).
37. Wolff, A.C. *et al.* Recommendations for human epidermal growth factor receptor 2 testing in breast cancer: American Society of Clinical Oncology/College of American Pathologists clinical practice guideline update. *Journal of clinical oncology : official journal of the American Society of Clinical Oncology* **31**, 3997-4013 (2013).
38. Lin, N.U. *et al.* Clinicopathologic features, patterns of recurrence, and survival among women with triple-negative breast cancer in the National Comprehensive Cancer Network. *Cancer* **118**, 5463-5472 (2012).
39. Lehmann, B.D. *et al.* Identification of human triple-negative breast cancer subtypes and preclinical models for selection of targeted therapies. *The Journal of clinical investigation* **121**, 2750-2767 (2011).
40. Lehmann, B.D. *et al.* Refinement of Triple-Negative Breast Cancer Molecular Subtypes: Implications for Neoadjuvant Chemotherapy Selection. *PloS one* **11**, e0157368 (2016).
41. Foulkes, W.D., Smith, I.E. & Reis-Filho, J.S. Triple-negative breast cancer. *The New England journal of medicine* **363**, 1938-1948 (2010).
42. Traina, T.A. *et al.* Enzalutamide for the Treatment of Androgen Receptor-Expressing Triple-Negative Breast Cancer. *Journal of clinical oncology : official journal of the American Society of Clinical Oncology* **36**, 884-890 (2018).
43. Robson, M. *et al.* Olaparib for Metastatic Breast Cancer in Patients with a Germline BRCA Mutation. *The New England journal of medicine* **377**, 523-533 (2017).

44. Amara, D. *et al.* Co-expression modules identified from published immune signatures reveal five distinct immune subtypes in breast cancer. *Breast cancer research and treatment* **161**, 41-50 (2017).
45. Denkert, C., Liedtke, C., Tutt, A. & von Minckwitz, G. Molecular alterations in triple-negative breast cancer-the road to new treatment strategies. *Lancet* **389**, 2430-2442 (2017).
46. Barbie, T.U. *et al.* Targeting an IKBKE cytokine network impairs triple-negative breast cancer growth. *The Journal of clinical investigation* **124**, 5411-5423 (2014).
47. Hoesel, B. & Schmid, J.A. The complexity of NF-kappaB signaling in inflammation and cancer. *Molecular cancer* **12**, 86 (2013).
48. Tornatore, L., Thotakura, A.K., Bennett, J., Moretti, M. & Franzoso, G. The nuclear factor kappa B signaling pathway: integrating metabolism with inflammation. *Trends Cell Biol* **22**, 557-566 (2012).
49. Israel, A. The IKK complex, a central regulator of NF-kappaB activation. *Cold Spring Harb Perspect Biol* **2**, a000158 (2010).
50. Wu, D. *et al.* NF-kappaB Expression and Outcomes in Solid Tumors: A Systematic Review and Meta-Analysis. *Medicine* **94**, e1687 (2015).
51. Liu, M. *et al.* The canonical NF-kappaB pathway governs mammary tumorigenesis in transgenic mice and tumor stem cell expansion. *Cancer Res* **70**, 10464-10473 (2010).
52. Hernandez, C., Huebener, P. & Schwabe, R.F. Damage-associated molecular patterns in cancer: a double-edged sword. *Oncogene* **35**, 5931-5941 (2016).
53. Rabouille, C. Pathways of Unconventional Protein Secretion. *Trends Cell Biol* **27**, 230-240 (2017).
54. Murshid, A., Theriault, J., Gong, J. & Calderwood, S.K. Investigating receptors for extracellular heat shock proteins. *Methods in molecular biology* **787**, 289-302 (2011).
55. Campisi, J., Leem, T.H. & Fleshner, M. Stress-induced extracellular Hsp72 is a functionally significant danger signal to the immune system. *Cell stress & chaperones* **8**, 272-286 (2003).
56. Fong, J.J. *et al.* Immunomodulatory activity of extracellular Hsp70 mediated via paired receptors Siglec-5 and Siglec-14. *The EMBO journal* **34**, 2775-2788 (2015).
57. Hance, M.W. *et al.* Secreted Hsp90 is a novel regulator of the epithelial to mesenchymal transition (EMT) in prostate cancer. *The Journal of biological chemistry* **287**, 37732-37744 (2012).
58. Kottke, T. *et al.* Induction of hsp70-mediated Th17 autoimmunity can be exploited as immunotherapy for metastatic prostate cancer. *Cancer Res* **67**, 11970-11979 (2007).
59. Nolan, K.D., Franco, O.E., Hance, M.W., Hayward, S.W. & Isaacs, J.S. Tumor-secreted Hsp90 subverts polycomb function to drive prostate tumor growth and invasion. *The Journal of biological chemistry* **290**, 8271-8282 (2015).
60. Salari, S. *et al.* Extracellular HSP27 acts as a signaling molecule to activate NF-kappaB in macrophages. *Cell stress & chaperones* **18**, 53-63 (2013).
61. Sims, J.D., McCready, J. & Jay, D.G. Extracellular heat shock protein (Hsp)70 and Hsp90alpha assist in matrix metalloproteinase-2 activation and breast cancer cell migration and invasion. *PloS one* **6**, e18848 (2011).
62. Theriault, J.R., Mambula, S.S., Sawamura, T., Stevenson, M.A. & Calderwood, S.K. Extracellular HSP70 binding to surface receptors present on antigen presenting cells and endothelial/epithelial cells. *FEBS letters* **579**, 1951-1960 (2005).
63. Thuringer, D. *et al.* Extracellular HSP27 mediates angiogenesis through Toll-like receptor 3. *FASEB journal : official publication of the Federation of American Societies for Experimental Biology* **27**, 4169-4183 (2013).
64. Tsutsumi, S. & Neckers, L. Extracellular heat shock protein 90: a role for a molecular chaperone in cell motility and cancer metastasis. *Cancer science* **98**, 1536-1539 (2007).
65. Wong, D.S. & Jay, D.G. Emerging Roles of Extracellular Hsp90 in Cancer. *Advances in cancer research* **129**, 141-163 (2016).

66. Stangl, S. *et al.* Targeting membrane heat-shock protein 70 (Hsp70) on tumors by cmHsp70.1 antibody. *Proceedings of the National Academy of Sciences of the United States of America* **108**, 733-738 (2011).
67. Wang, X. *et al.* The regulatory mechanism of Hsp90alpha secretion and its function in tumor malignancy. *Proceedings of the National Academy of Sciences of the United States of America* **106**, 21288-21293 (2009).
68. Ulmansky, R. *et al.* A Humanized Monoclonal Antibody against Heat Shock Protein 60 Suppresses Murine Arthritis and Colitis and Skews the Cytokine Balance toward an Anti-Inflammatory Response. *Journal of immunology* **194**, 5103-5109 (2015).
69. Fusella, F. *et al.* Morgana acts as a proto-oncogene through inhibition of a ROCK-PTEN pathway. *J Pathol* **234**, 152-163 (2014).
70. Kessenbrock, K., Plaks, V. & Werb, Z. Matrix metalloproteinases: regulators of the tumor microenvironment. *Cell* **141**, 52-67 (2010).
71. Yousef, E.M., Tahir, M.R., St-Pierre, Y. & Gaboury, L.A. MMP-9 expression varies according to molecular subtypes of breast cancer. *BMC cancer* **14**, 609 (2014).
72. Chen, G., Cao, P. & Goeddel, D.V. TNF-induced recruitment and activation of the IKK complex require Cdc37 and Hsp90. *Mol Cell* **9**, 401-410 (2002).
73. Viatour, P., Merville, M.P., Bours, V. & Chariot, A. Phosphorylation of NF-kappaB and IkappaB proteins: implications in cancer and inflammation. *Trends in biochemical sciences* **30**, 43-52 (2005).
74. Morvan, M.G. & Lanier, L.L. NK cells and cancer: you can teach innate cells new tricks. *Nat Rev Cancer* **16**, 7-19 (2016).
75. Puchalapalli, M. *et al.* NSG Mice Provide a Better Spontaneous Model of Breast Cancer Metastasis than Athymic (Nude) Mice. *PloS one* **11**, e0163521 (2016).
76. Coffelt, S.B., Wellenstein, M.D. & de Visser, K.E. Neutrophils in cancer: neutral no more. *Nat Rev Cancer* **16**, 431-446 (2016).
77. Coffelt, S.B. *et al.* IL-17-producing gammadelta T cells and neutrophils conspire to promote breast cancer metastasis. *Nature* **522**, 345-348 (2015).
78. Wculek, S.K. & Malanchi, I. Neutrophils support lung colonization of metastasis-initiating breast cancer cells. *Nature* **528**, 413-417 (2015).
79. Martin, M., Wei, H. & Lu, T. Targeting microenvironment in cancer therapeutics. *Oncotarget* **7**, 52575-52583 (2016).
80. Feizi, A., Banaei-Esfahani, A. & Nielsen, J. HCSD: the human cancer secretome database. *Database : the journal of biological databases and curation* **2015**, bav051 (2015).
81. Bendtsen, J.D., Jensen, L.J., Blom, N., Von Heijne, G. & Brunak, S. Feature-based prediction of non-classical and leaderless protein secretion. *Protein engineering, design & selection : PEDS* **17**, 349-356 (2004).
82. Obenauer, J.C., Cantley, L.C. & Yaffe, M.B. Scansite 2.0: proteome-wide prediction of cell signaling interactions using short sequence motifs. *Nucleic Acids Research* **31**, 3635-3641 (2003).
83. Mamat, U. *et al.* Endotoxin-free protein production—ClearColi™ technology. *Nature Methods* **10**, 916 (2013).
84. Huang, B., Zhao, J., Unkeless, J.C., Feng, Z.H. & Xiong, H. TLR signaling by tumor and immune cells: a double-edged sword. *Oncogene* **27**, 218 (2008).
85. McAllister, S.S. & Weinberg, R.A. The tumour-induced systemic environment as a critical regulator of cancer progression and metastasis. *Nature cell biology* **16**, 717-727 (2014).
86. Gajewski, T.F., Schreiber, H. & Fu, Y.X. Innate and adaptive immune cells in the tumor microenvironment. *Nature immunology* **14**, 1014-1022 (2013).
87. Peinado, H. *et al.* Pre-metastatic niches: organ-specific homes for metastases. *Nat Rev Cancer* **17**, 302-317 (2017).

88. Thuringer, D. *et al.* Transactivation of the epidermal growth factor receptor by heat shock protein 90 via Toll-like receptor 4 contributes to the migration of glioblastoma cells. *The Journal of biological chemistry* **286**, 3418-3428 (2011).
89. Stellas, D., Karameris, A. & Patsavoudi, E. Monoclonal antibody 4C5 immunostains human melanomas and inhibits melanoma cell invasion and metastasis. *Clin Cancer Res* **13**, 1831-1838 (2007).
90. Tsutsumi, S. *et al.* A small molecule cell-impermeant Hsp90 antagonist inhibits tumor cell motility and invasion. *Oncogene* **27**, 2478-2487 (2008).
91. Bhatelia, K., Singh, K. & Singh, R. TLRs: linking inflammation and breast cancer. *Cellular signalling* **26**, 2350-2357 (2014).
92. Theodoropoulos, G.E. *et al.* Toll-like receptors gene polymorphisms may confer increased susceptibility to breast cancer development. *Breast* **21**, 534-538 (2012).
93. Kaczanowska, S., Joseph, A.M. & Davila, E. TLR agonists: our best frenemy in cancer immunotherapy. *Journal of leukocyte biology* **93**, 847-863 (2013).
94. Tsan, M.F. & Gao, B. Heat shock proteins and immune system. *Journal of leukocyte biology* **85**, 905-910 (2009).

Publications

Brancaccio M, Rocca S, Seclì L, Busso E, Fusella F. The double face of Morgana in tumorigenesis. Oncotarget. 2015 Dec

Fusella F*, Seclì L*, Busso E, Krepelova A, Moiso E, Rocca S, Conti L, Annaratone L, Rubinetto C, Mello-Grand M, Singh V, Chiorino G, Silengo L, Altruda F, Turco E, Morotti A, Oliviero S, Castellano I, Cavallo F, Provero P, Tarone G, Brancaccio M. The IKK/NF-κB signaling pathway requires Morgana to drive breast cancer metastasis. Nat Commun. 2017 Nov

Fusella F, Seclì L, Brancaccio M. Escaping NK cells and recruiting neutrophils: How Morgana/NF-κB signaling promotes metastasis. Mol Cell Oncol. 2018 Jan